# Joint Preprocesser-Based Detectors for One-Way and Two-Way Cooperative Communication Networks

Thesis by

**Abdulrahman Issam Taher Abuzaid**

In Partial Fulfillment of the Requirements

For the Degree of

**Master of Science**

**in Electrical Engineering**

King Abdullah University of Science and Technology, Thuwal,

Kingdom of Saudi Arabia

(May, 2014)

The thesis of Abdulrahman Issam Taher Abuzaid is approved by the examination committee

Committee Chairperson: Mohamed-Slim Alouini

Committee Member: Tareq Al-Naffouri

Committee Member: Taous-Meriem Laleg

# ABSTRACT

Joint Preprocesser-Based Detectors for One-Way and Two-Way Cooperative Communication Networks

Abdulrahman Issam Taher Abuzaid

Efficient receiver designs for cooperative communication systems are becoming increasingly important. In previous work, cooperative networks communicated with the use of $L$ relays. As the receiver is constrained, channel shortening and reduced-rank techniques were employed to design the preprocessing matrix that reduces the length of the received vector from $L$ to $U$. In the first part of the work, a receiver structure is proposed which combines our proposed threshold selection criteria with the joint iterative optimization (JIO) algorithm that is based on the mean square error (MSE). Our receiver assists in determining the optimal $U$. Furthermore, this receiver provides the freedom to choose $U$ for each frame depending on the tolerable difference allowed for MSE. Our study and simulation results show that by choosing an appropriate threshold, it is possible to gain in terms of complexity savings while having no or minimal effect on the BER performance of the system. Furthermore, the effect of channel estimation on the performance of the cooperative system is investigated. In the second part of the work, a joint preprocessor-based detector for cooperative communication networks is proposed for one-way and two-way relaying. This joint preprocessor-based detector operates on the principles of minimizing the symbol error rate (SER) instead of minimizing MSE. For a realistic assessment,

pilot symbols are used to estimate the channel. From our simulations, it can be observed that our proposed detector achieves the same SER performance as that of the maximum likelihood (ML) detector with all participating relays. Additionally, our detector outperforms selection combining (SC), channel shortening (CS) scheme and reduced-rank techniques when using the same $U$. Finally, our proposed scheme has the lowest computational complexity.

# ACKNOWLEDGEMENTS

First of all, I would like to thank Dr. Qasim Zeeshan Ahmed for his continuous help and patience over the past year. The numerous discussions we had made this work possible. I would also like to thank Prof. Mohamed-Slim Alouini for his incessant encouragement and his helpful advice throughout my studies at KAUST. I am also indebted to Prof. Tareq Al-Naffouri and Prof. Taous-Meriem Laleg for their helpful comments regarding my work.

Finally, I would like to thank my parents and all of my brothers and sisters, without them I would not have been able to accomplish this and reach where I am today.

# LIST OF SYMBOLS

| Symbol | Description |
|---|---|
| $L$ | Number of relays |
| $U$ | Number of relays used in the reduced-rank system |
| $\mathbf{A}^*$ | Complex conjugate of arbitrary matrix $\mathbf{A}$ |
| $\mathbf{A}^T$ | Transpose of arbitrary matrix $\mathbf{A}$ |
| $\mathbf{A}^H$ | Hermitian of arbitrary matrix $\mathbf{A}$ |
| $\mathbf{A}^{-1}$ | Inverse of arbitrary matrix $\mathbf{A}$ |
| $E[\cdot]$ | Expectation operation |
| $\text{diag}[\cdot]$ | Diagonal matrix |
| $\lvert \cdot \rvert$ | Absolute value |
| $R_l$ | $l$-th relay |
| $S$ | Source |
| $D$ | Destination |
| $h_{SR_l}$,$\sigma^2_{h_{SR_l}}$ | The channel from $S$ to the $l$th relay and its variance |
| $h_{R_lD}$,$\sigma^2_{h_{R_lD}}$ | The channel from the $l$th relay to $D$ and its variance |
| $h_{DR_l}$,$\sigma^2_{h_{DR_l}}$ | The channel from $D$ to the $l$th relay and its variance |
| $h_{R_lS}$,$\sigma^2_{h_{R_lS}}$ | The channel from the $l$th relay to $S$ and its variance |
| $n_{R_l}$,$\sigma^2_{R_l}$ | AWGN noise added at the $l$th relay and its variance |
| $\zeta_{R_l}$ | Amplification factor at the $l$-th relay |

| Symbol | Description |
|---|---|
| $\boldsymbol{y}$ | Overall received signal in vector format |
| $\boldsymbol{w}$ | Linear weight vector of size $L$ |
| $\bar{\boldsymbol{w}}$ | Linear reduced-rank weight vector of size $U$ |
| $\boldsymbol{P}$ | Pre-processing matrix of size $L \times U$ |
| $\boldsymbol{R}$ | The autocorrelation matrix of size $L \times L$ |
| $\boldsymbol{\rho}$ | the cross-correlation between $\boldsymbol{y}$ and $x$ |
| $n_{D_l}$,$\sigma_D^2$ | AWGN noise added at the destination $D$ and its variance |
| $\epsilon_{h_l}$ | Channel estimation error |
| $\hat{h}$ | Estimated channel |
| $\boldsymbol{\Sigma}$ | noise covariance |
| $x_1$ | transmitted signal by $S$ |
| $x_2$ | transmitted signal by $D$ |
| $\mu$ | Step-size of steepest descent algorithm for $\boldsymbol{w}$ |
| $\eta$ | Step-size of steepest descent algorithm for $\boldsymbol{P}$ |

# LIST OF ABBREVIATIONS

| Symbol | Meaning |
|---|---|
| AWGN | Additive White Gaussian Noise |
| AF | Amplify-and-Forward |
| BER | Bit-Error Rate |
| BPSK | Binary Phase Shift Keying |
| CS | Channel Shortening |
| CSI | Channel State Information |
| CSM | Cross Spectral Metric |
| DF | Decode-and-Forward |
| JIO | Joint Iterative Optimzation |
| MBER | Minimum Bit-Error Rate |
| MMSE | Minimum Mean-Square Error |
| ML | Maximum Liklihood |
| MRC | Maximal Ratio Combining |
| MSE | Mean-Square Error |
| MSER | Minimum Symbol-Error Rate |
| MSWF | Multi-Stage Wiener Filter |
| OWR | One-Way Relaying |
| PC | Principal Component |
| PDF | Probability Density Function |
| QAM | Quadrature Amplitude Modulation |
| QPSK | Quadrature Phase Shift Keying |
| SC | Selection Combining |
| SD | Steepest Descent |
| SNR | Signal-to-Noise Ratio |
| TPA | Taylor Polynomial Approximation |
| TWR | Two-Way Relaying |

# TABLE OF CONTENTS

# LIST OF FIGURES

# LIST OF TABLES

# Chapter 1

# Introduction

## 1.1 Cooperative Communication Systems

Cooperative Communications is a new scheme to achieve spatial diversity in communication systems that lack multi antennas. The basic idea is that when different users have independent information, and when a relay has periods of inactivity, other users can exploit these inactive periods to send their data through the inactive relay. Because of omnidirectional antennas, the users do not need to transmit with higher power, but the helping relay will need to use more energy to transmit its data and the data of the helped users. This does not necessarily increase the overall network consumption of energy since the users can now reduce their transmitting power and still achieve the same performance because of the higher order of diversity [1].

Two different possibilities for the relays are either to amplify-and-forward (AF) the data or decode-and-forward (DF) the data. AF amplifies the signal with its noise and forwards it to the destination transceiver while DF decodes it first and as a result cleans it from noise and then forwards it. DF adds more complexity to the relays and often will not be necessary as AF has acceptable performance [2].

To explain the difference between one-way and two-way relaying, let us assume a system with two users and a relay in between. The end-to-end transmission of

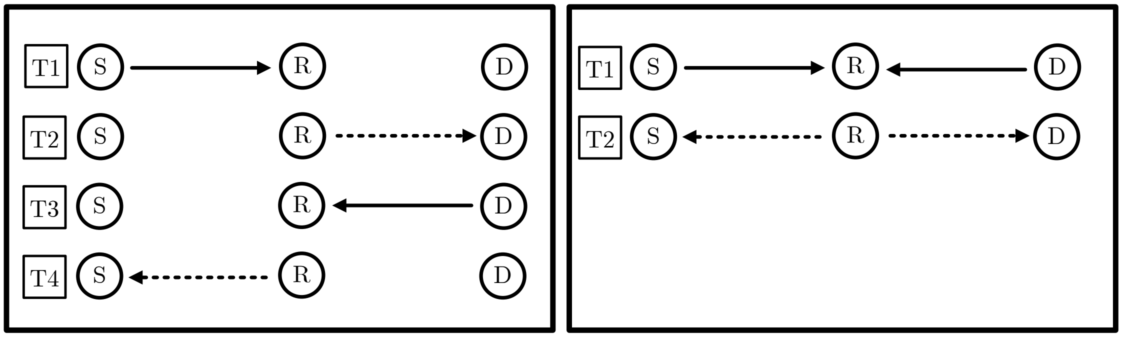


(a) Four time slots for one-way relaying

(b) Two time slots for two-way relaying

Figure 1.1: Cooperative communications for a system of 1 relay and across the different time slots. (a) One-way relaying, (b) Two-way relaying.

data has two possibilities. The first user can send its data to the relay and the relay forwards it to the second user. Once the data is received, the second user sends its data to the relay and the relay forwards it to the first user. This is what is called a unidirectional transmission or one-way relaying. From this description, it is clear that the system will require four time slots to exchange data between the two users. The other possibility is that both users send their data to the relay, where it gets combined, amplified, and transmitted back to the users. This alternative system requires two time slots and hence will improve the overall system spectral efficiency [3]. The difference between one-way and two-way relaying is accentuated in Fig. 1.1.

## 1.2 An Overview of Classic Detectors

The maximum-likelihood (ML) detector, the minimum mean-square error (MMSE) detector, and the maximal-ratio combining (MRC) detector are extensively used in this thesis as benchmarks for our adaptive detectors. In this section, we briefly introduce these detector for a hypothetical system model with a received signal $\boldsymbol{y}$ of size $L \times 1$ and carrying information about a transmitted symbol $x$, and finally having a noise variance matrix $\mathbf{\Sigma}$ of size $L \times L$.

### 1.2.1 Maximum-Likelihood Detection

The ML detector requires knowledge of the covariance matrix, and in cases of independent L paths, it becomes a diagonal matrix $\boldsymbol{\Sigma}$ that has $\sigma_l^2$ as the diagonal elements. But our discussion here applies to any random noise variance matrix. The received vector's probability density function can be represented as a complex Gaussian as follows

$$f(\boldsymbol{y}|x_i, \boldsymbol{h}) = \frac{1}{\pi^L} e^{-(\boldsymbol{y}-\boldsymbol{h}x_i)^H \boldsymbol{\Sigma}^{-1} (\boldsymbol{y}-\boldsymbol{h}x_i)}. \tag{1.1}$$

In order to make a decision that a certain symbol $x_i$ was sent, we need

$$f(\boldsymbol{y}|x_i, \boldsymbol{h}) > f(\boldsymbol{y}|x_j, \boldsymbol{h}), \quad \forall j \neq i, \tag{1.2}$$

to be true, or equivalently

$$(\boldsymbol{y} - \boldsymbol{h}x_i)^H \boldsymbol{\Sigma}^{-1} (\boldsymbol{y} - \boldsymbol{h}x_i) < (\boldsymbol{y} - \boldsymbol{h}x_j)^H \boldsymbol{\Sigma}^{-1} (\boldsymbol{y} - \boldsymbol{h}x_j), \quad \forall j \neq i. \tag{1.3}$$

If BPSK is used, $x_i$ has only two possibilities $\pm 1$, meaning that a single comparison is sufficient to detect a symbol. One of the drawbacks of this method is that for a constellation with a large $M$, where $M$ is the constellation size, the number of calculations can grow quickly.

### 1.2.2 Maximal Ratio Combining

The MRC scheme assumes that the L observations can be linearly combined with the help of a filter, $\boldsymbol{w}$. It is found that the linear filter that maximizes the signal-to-noise

(SNR) ratio is given as

$$\boldsymbol{w} = \boldsymbol{h}. \tag{1.4}$$

To prove this, consider the linear filter $w$ when applied to our received vector, more explicitly

$$\sum_{l=1}^{L} w_l y_l = x \sum_{l=1}^{L} w_l h_l + \sum_{l=1}^{L} w_l n_l. \tag{1.5}$$

Reducing the bit error rate requires maximizing the instantaneous SNR

$$SNR_{inst.} = \frac{|x|^2 |\sum_{l=1}^{L} w_l h_l|^2}{\mathbf{E}(\sum_{l=1}^{L} w_l n_l)} \tag{1.6}$$

$$SNR_{inst.} = \frac{|x|^2 |\sum_{l=1}^{L} w_l h_l|^2}{\sum_{l=1}^{L} |w_l|^2}. \tag{1.7}$$

Using the Cauchy Schwarz inequality, which states that

$$|\sum_{l=1}^{L} w_l h_l|^2 \leq \sum_{l=1}^{L} |w_l|^2 . \sum_{l=1}^{L} |h_l|^2, \tag{1.8}$$

with equality only when $w_l$ and $h_l^*$ are linearly dependent. In other words, to use MRC detection, every $y_l$ observation must be multiplied by $h_l^*$ and then by summing over all the elements we get a scalar that can be used to detect the symbol transmitted.

### 1.2.3 Minimum Mean Square Error Detector

MMSE is another scheme to design the linear filter $w$ that combines the observations. The mean square error cost function is to be minimized

$$\begin{aligned} J(\boldsymbol{w}) = E(|x - \boldsymbol{w}^H\boldsymbol{y}|^2) &= E[(x - \boldsymbol{w}^H\boldsymbol{y})(x - \boldsymbol{w}^H\boldsymbol{y})^H] \\ &= E[(x - \boldsymbol{w}^H\boldsymbol{y})(x^* - \boldsymbol{y}^H\boldsymbol{w})] \\ &= E(xx^* - x\boldsymbol{y}^H\boldsymbol{w} - \boldsymbol{w}^H\boldsymbol{y}x^* + \boldsymbol{w}^H\boldsymbol{y}\boldsymbol{y}^H\boldsymbol{w}) \\ &= E(xx^*) - E(x\boldsymbol{y}^H)\boldsymbol{w} - \boldsymbol{w}^H E(\boldsymbol{y}x^*) + \boldsymbol{w}^H E(\boldsymbol{y}\boldsymbol{y}^H)\boldsymbol{w} \\ &= \sigma_x^2 - \boldsymbol{\rho}^H\boldsymbol{w} - \boldsymbol{w}^H\boldsymbol{\rho} + \boldsymbol{w}^H R\boldsymbol{w}, \end{aligned} \tag{1.9}$$

where $\sigma_x^2 = E(xx^*)$, $\boldsymbol{\rho} = E(\boldsymbol{y}x^*)$, and $\boldsymbol{R} = E(\boldsymbol{y}\boldsymbol{y}^H)$. By differentiating with respect to $\boldsymbol{w}$ and equating to zero we can find the optimum weight vector

$$\begin{aligned} \nabla_{\boldsymbol{w}} J &= 0 - \boldsymbol{\rho} - \boldsymbol{\rho} + 2\boldsymbol{R}\boldsymbol{w}_o \\ &= 2\boldsymbol{\rho} + 2\boldsymbol{R}\boldsymbol{w}_o \\ \boldsymbol{w}_o &= \boldsymbol{R}^{-1}\boldsymbol{\rho}. \end{aligned} \tag{1.10}$$

Proceeding to get $\boldsymbol{w}_o$ in terms of the channels and the noise matrix $\Sigma$

$$\begin{aligned} \boldsymbol{R} &= E(\boldsymbol{y}\boldsymbol{y}^H) \\ &= E[(\boldsymbol{h}x + \boldsymbol{n})(\boldsymbol{h}x + \boldsymbol{n})^H] \\ &= E[(\boldsymbol{h}x + \boldsymbol{n})(\boldsymbol{h}^H x^* + \boldsymbol{n}^H)] \\ &= E(\boldsymbol{h}xx^*\boldsymbol{h}^H + \boldsymbol{h}x\boldsymbol{n}^H + \boldsymbol{n}x^*\boldsymbol{h}^H + \boldsymbol{n}\boldsymbol{n}^H) \\ &= \boldsymbol{h}E(xx^*)\boldsymbol{h}^H + \boldsymbol{h}E(x\boldsymbol{n}^H) + E(\boldsymbol{n}x^*)\boldsymbol{h}^H + E(\boldsymbol{n}\boldsymbol{n}^H) \\ &= \boldsymbol{h}I\boldsymbol{h}^H + 0 + 0 + \boldsymbol{\Sigma} \\ &= \boldsymbol{h}\boldsymbol{h}^H + \boldsymbol{\Sigma}, \end{aligned} \tag{1.11}$$

since $E(x) = 0$, $E(\boldsymbol{n}) = \mathbf{0}$, and $E(x\boldsymbol{n}) = E(x)E(\boldsymbol{n})$. The cross correlation vector $\boldsymbol{\rho}$ can also be determined as follows

$$\begin{aligned}\boldsymbol{\rho} &= E(\boldsymbol{y}x^*)\\ &= E[(\boldsymbol{h}x + \boldsymbol{n})x^*]\\ &= E(\boldsymbol{h}xx^* + \boldsymbol{n}x^*)\\ &= \boldsymbol{hI} + 0\\ &= \boldsymbol{h}. \qquad (1.12)\end{aligned}$$

Finally, the overall expression for the optimum weight vector reduces to

$$\boldsymbol{w}_o = (\boldsymbol{h}\boldsymbol{h}^H + \boldsymbol{\Sigma})^{-1}\boldsymbol{h}. \qquad (1.13)$$

## 1.3 Literature Review

Network coverage, bit error rate (BER) performance, and battery life are important parameters when designing a cooperative network [4]. Usually, relays are operated by batteries and have small coverage range [5–8]. Cooperative diversity allows multiple relays to form a virtual antenna array resulting in spatial diversity and improved network coverage and performance [4, 9]. This improved coverage results in higher complexity which results in battery drain, despite adopting amplify-and-forward (AF) (which is the most efficient in terms of battery life compared to decode-and-forward (DF)) [2, 8].

For relay networks with $L$ relays, selection combining is thought of as a solution to the higher complexity problem [10]. The $U$ relays with the highest signal-to-noise ratio (SNR) are selected and all the power budget is directed to those relays. The selected $U$ relays now transmit the information with a power equivalent to $L$

relays [10]. The relays are operated with the help of batteries and it is not a feasible solution to transmit the signal with more power. Therefore, selecting the best relay is not a suitable solution. In order to solve this issue, a solution based on channel-shortening (CS) is proposed in [11]. A preprocessing matrix is designed which picks $U$ out of $L$ relays based on channel shortening principles. This scheme outperforms selection combining but wastes the energy of $(L - U)$ relays. Recently in [12], a preprocessing matrix that uses reduced-rank principles is proposed. It is shown that designing the preprocessing matrix with the help of a reduced-rank will extract the energy from all the $L$ relays, while still maintaining a lower complexity and achieving the same BER performance as all participating relays. All the above schemes have a fixed $U$ and require channel state information (CSI). In practice, perfect channel knowledge is very hard to acquire and channel estimation will be noisy. Therefore, in this thesis, channel estimation error is introduced when designing the receiver for cooperative communications. Recently, to address this problem, the impact of imperfect CSI on several research topics has been studied in [13–16]. Keeping in view with the above mentioned issues, in this thesis, a joint iterative optimization (JIO) algorithm is adopted [17, 18]. However, two main problems still persist that will be discussed in the first part of our work: a) determining the optimized $U_{opt}$ b) reducing the computational complexity without affecting the MSE performance or with minimal effect on MSE.

A myriad of detectors have been proposed when the channel state information (CSI) is known; such as selection combining (SC) [10], channel shortening (CS) [11], principal component (PC) [19], cross spectral metric (CSM) [20], and Taylor polynomial approximation (TPA)-based minimum mean square error (MMSE) [12], also known as multi-stage wiener filter (MSWF) [17]. When employing variable gain amplification factor at the relays, it was observed that for a given $U$, TPA-based technique significantly outperforms the PC-, CSM-, and CS-assisted techniques. However, in order to achieve the performance of all participating relays the value of $U$ needs to comparatively high. Therefore, the motivation for our present work is to design a detector which achieves similar performance as all participating relays but with a lower $U$.

A lot of work have been done in the area of two-way relaying (TWR). TWR helps increase the system's spectral efficiency, as this result was proved in various papers in the literature [3,21–23]. The overall outage probability and symbols error probability for TWR were studied in detail in [23,24]. Also in [25], it was shown that when there is large path loss attenuation, TWR not only has higher spectral efficiency but also has higher energy efficiency than one-way relaying (OWR).

In this thesis, a new detector is proposed for cooperative communication systems which operates on the principles of minimum symbol error rate (MSER). The proposed algorithm now minimizes the probability of error, which is superior to minimizing the mean square error [26–29], by jointly designing the weights of the filter and the preprocessing matrix. It can be observed from the simulations that this detector is able to achieve the same SER performance as all participating relays and always outperform the TPA-based MMSE detector for the same $U$. Furthermore, by designing this preprocessing matrix, the detector now can operate with filters of long lengths [30]. As most of the literature in cooperative communication assume perfect channel knowledge at the receiver side, this assumption is replaced with the estimation of the channel with the assistance of pilot symbols [31]. This assumption was first introduced by [32, 33], however, both these references used the MSE criteria. Therefore, at the receiver side we will have imperfect channel knowledge due to imperfect channel estimation.

## 1.4 Objectives and Contributions

The contributions of this thesis can be summarized in the following points:

• An algorithm based on minimum mean square error (MMSE) is designed for determining the best $U$ for each data frame instead of using unnecessarily large $U$.

• The algorithm is able to achieve the same MSE performance of the classic JIO algorithm but with lower computational complexity.

• This algorithm further trades the MSE by using a threshold $\delta$, which results in comparable MSE performance but much lower complexity.

• Our study and simulation results show that with our proposed detector it is possible to gain in terms of complexity savings without affecting the BER performance of the system. Opting for a $U$ that is lower than the best for each frame will achieve comparable BER performance but with more computational savings.

• In scenarios where the exact channel knowledge is not available, this algorithm is able to achieve similar performance as all participating relays whether there is a small or a large estimation error.

• A joint preprocessor-based MSER detector (JP-MSER) is proposed for systems which are limited in training length.

• A new preprocessor matrix is designed based on minimizing the SER for the detector.

• Similar performance as the ML detector is achieved by using our proposed detector with a lower computational complexity.

• Perfect channel knowledge at the receiver side is replaced by the estimated channel.

## 1.5 Outline of Thesis

Chapter 2 proposes a modified version of the JIO algorithm for one-way cooperative communication systems, where the detector is MSE-based. Chapter 3 proposes a new detector for one-way and two-way cooperative communication systems that minimizes the SER instead of the MSE and also discusses the design of its preprocessing matrix. Finally, Chapter 4 concludes the thesis and discusses various ideas for future work.

# Chapter 2

# Adaptive Detector Based on Minimum Mean Square Error Criteria

In this chapter, an algorithm based on minimum mean square error (MMSE) is designed for determining the best or optimized rank of the system $U$, which we denote $U_{opt}$ in our work. This $U_{opt}$ will be different for each data frame and is always less than or equivalent to the fixed $U_{max}$, where $U_{max}$ is the value of $U$ that is used in the classical JIO algorithm. The algorithm is able to achieve the same MSE performance as that of $U_{max}$ but with lower computational complexity. This algorithm further trades the MSE by using a threshold $\delta$, which results in comparable MSE performance but at a much lower complexity. Our study and simulation results show that, with our proposed detector, it is possible to gain in terms of complexity savings without affecting the BER performance of the system. Opting for a $U < U_{opt}$ will achieve comparable BER performance but with more computational savings. Furthermore, in scenarios where the exact channel knowledge is not available, this algorithm is able to achieve similar performance as all participating relays whether there is a small or a large estimation error.

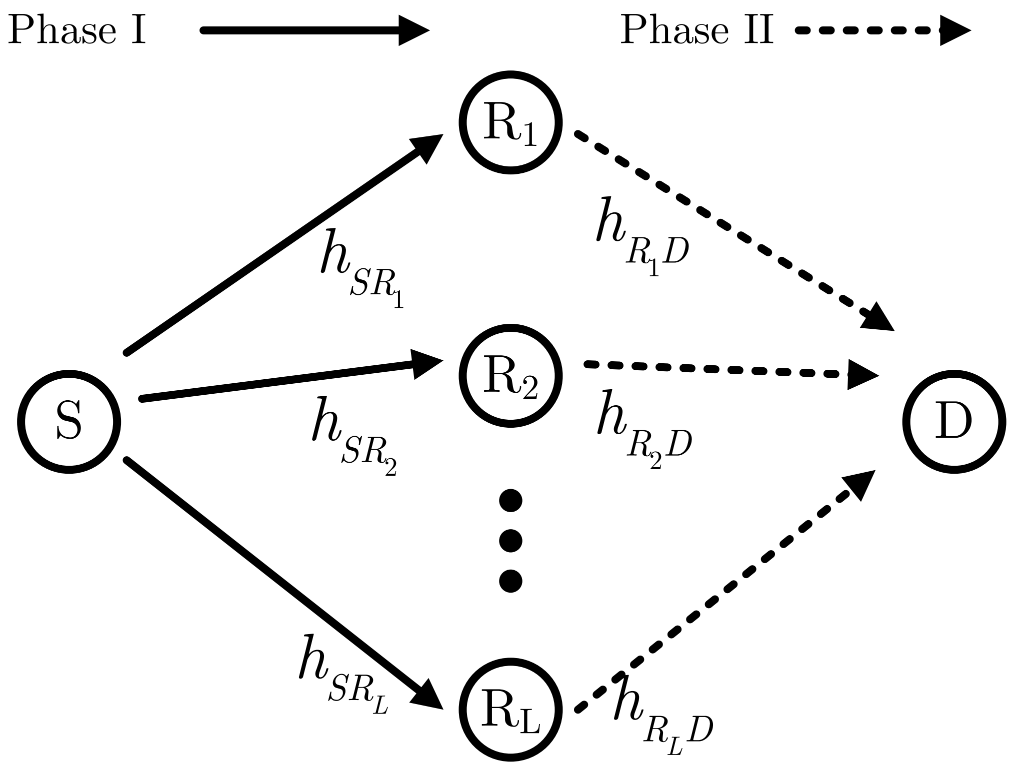


Figure 2.1: A typical one-way amplify-and-forward (AF) cooperative communication system with $L$ relays. A direct link is unavailable and each relay employs variable gain amplification.

## 2.1 System Model

The system model considered in this chapter is the same model used in [34] and is shown in Fig. 2.1. The source $S$ transmits its information symbol to the destination $D$ with the help of $L$ relays denoted by $R_l$ where $l = 1, 2, \ldots, L$. The transmission happens in two phases. In phase I, the source broadcasts the information to the $L$ relays, while in phase II the relays retransmit the data to the destination. A direct link between the source and the destination is ignored due to the large distance between $S$ and $D$. The channel between the source and the $l$th relay is complex Gaussian denoted by $h_{SR_l}$ with variance $\sigma^2_{h_{SR_l}}$, while the channel between the $l$th relay and the destination is complex Gaussian denoted by $h_{R_lD}$ with variance $\sigma^2_{h_{R_lD}}$. In order to mitigate interference and treat the channel as a single tap, orthogonality can be used in either frequency or time domain [12, 35]. As the exact channel knowledge is unavailable, we define the estimate of the channel $\hat{h}_{SR_l}$ and $\hat{h}_{R_lD}$ as [14–16]

$$h_{SR_l} = \hat{h}_{SR_l} + \epsilon_{SR_l}, \tag{2.1}$$

$$h_{R_lD} = \hat{h}_{R_lD} + \epsilon_{R_lD}, \tag{2.2}$$

where $\epsilon_{i_l}$ is the channel estimation error and is assumed to be complex Gaussian with mean zero and variance $\sigma^2_{\epsilon_{i_l}} = \sigma^2_{i_l} - \sigma^2_{\hat{i}_l}$. This variance of channel estimation error measures the quality of the channel estimator. Generally, for an accurate estimate this parameter should be 0. However, depending upon the channel dynamics and estimation techniques the variance of error might be large.

### 2.1.1 Phase-I: Transmission from the Source

In phase-I, the source $S$ broadcasts the symbol $x$ to the relays and the received signal at the $l$th relay is expressed as

$$\begin{aligned} y_{R_l} &= h_{SR_l}x + n_{R_l}, \quad l = 1, 2, \ldots, L, \\ &= \hat{h}_{SR_l}x + \epsilon_{SR_l}x + n_{R_l}, \quad l = 1, 2, \ldots, L, \end{aligned} \tag{2.3}$$

where $x$ has average energy $\sigma^2_x = \mathbf{E}[xx^*] = 1$, and $n_{R_l}$ denotes the complex additive white Gaussian noise (AWGN) added at the $l$th relay with zero mean and variance $\sigma^2_{R_l}$, i.e., depending upon the hardware, each relay might have a different variance.

### 2.1.2 Phase-II: Transmission from the Relay

In phase II, each relay amplifies its signal with an amplification factor $\zeta_{R_l}$ that enforces a unity long-term average [36]

$$\zeta_{R_l} = \sqrt{\frac{1}{|h_{SR_l}|^2 + \sigma^2_{\epsilon_{SR_l}} + \sigma^2_{R_l}}}, \quad l = 1, 2, \ldots, L. \tag{2.4}$$

The signal received by $D$, when treating $\zeta_{R_l} y_{R_l}$ as the new symbol to be transmitted by the relays to the destination, is written as

$$\begin{aligned} y_l &= h_{R_l D} \zeta_{R_l} y_{R_l} + n_{D_l} \\ &= \zeta_{R_l} h_{R_l D} h_{SR_l} x + \zeta_{R_l} h_{R_l D} n_{R_l} + n_{D_l} \\ &= \zeta_{R_l} \hat{h}_{R_l D} \hat{h}_{SR_l} x + \zeta_{R_l} (\hat{h}_{SR_l} \epsilon_{R_l D} + \hat{h}_{R_l D} \epsilon_{SR_l} + \epsilon_{SR_l} \epsilon_{R_l D}) x \\ &+ \zeta_{R_l} (\hat{h}_{R_l D} + \epsilon_{R_l D}) n_{R_l} + n_{D_l}, \quad l = 1, 2, \ldots, L, \end{aligned} \tag{2.5}$$

where $n_{D_l}$ is complex AWGN noise with zero mean and variance $\sigma^2_D$.

### 2.1.3 Receiver Structure

Finally, the received signal from all the relays can be expressed in vector form as

$$\boldsymbol{y} = \hat{\boldsymbol{h}} x + \boldsymbol{\epsilon} x + \boldsymbol{n}, \tag{2.6}$$

where

$$\hat{\boldsymbol{h}} = \begin{bmatrix} \zeta_{R_1} \hat{h}_{R_1 D} \hat{h}_{SR_1} \\ \vdots \\ \zeta_{R_L} \hat{h}_{R_L D} \hat{h}_{SR_L} \end{bmatrix}, \quad \boldsymbol{n} = \begin{bmatrix} \zeta_{R_1} (\hat{h}_{R_1 D} + \epsilon_{R_1 D}) n_{R_1} + n_{D_1} \\ \vdots \\ \zeta_{R_L} (\hat{h}_{R_L D} + \epsilon_{R_L D}) n_{R_L} + n_{D_L} \end{bmatrix},$$

$$\boldsymbol{\epsilon} = \begin{bmatrix} \zeta_{R_1}(\hat{h}_{SR_1}\epsilon_{R_1D} + \hat{h}_{R_1D}\epsilon_{SR_1} + \epsilon_{SR_1}\epsilon_{R_1D}) \\ \vdots \\ \zeta_{R_L}(\hat{h}_{SR_L}\epsilon_{R_LD} + \hat{h}_{R_LD}\epsilon_{SR_L} + \epsilon_{SR_L}\epsilon_{R_LD}) \end{bmatrix}. \tag{2.7}$$

The model of (2.6) is equivalent to a known channel with information-dependent and non-Gaussian noise terms. Under the assumption that the noise term and information dependent terms are independent, the covariance of the total noise $\mathbf{\Sigma}$ is represented as

$$\mathbf{\Sigma} = E[\boldsymbol{n}\boldsymbol{n}^H + \boldsymbol{\epsilon}\boldsymbol{\epsilon}^H], \tag{2.8}$$

where $\mathbf{\Sigma}$ is a matrix of size $(L \times L)$. In situations where we assume independent noise terms and zero channel estimation error variance, $\mathbf{\Sigma}$ becomes a diagonal matrix of size $L$ and is represented as

$$\mathbf{\Sigma} = \text{diag}[\sigma_1^2, \sigma_2^2, \ldots, \sigma_L^2], \tag{2.9}$$

where $\sigma_l^2$ is given as

$$\begin{aligned} \sigma_l^2 &= \zeta_{R_l}^2|h_{R_lD}|^2\sigma_{R_l}^2 + \sigma_D^2 \\ &= \frac{|h_{R_lD}|^2\sigma_{R_l}^2}{|h_{SR_l}|^2 + \sigma_{R_l}^2} + \sigma_D^2. \end{aligned} \tag{2.10}$$

Let us now proceed towards the problem formulation and previous work carried out in the upcoming section.

## 2.2 Problem Formulation and Previous Work

For equally likely symbols, the maximum-likelihood (ML) detector is the optimal detector in terms of BER performance [37]. The High computational complexity of the ML detector motivated researchers to investigate a number of suboptimal detectors. The minimum mean square error (MMSE) has a near optimal performance, as it minimizes the mean square error (MSE) between the filter output and the information symbol. For the MMSE detector, the optimal weight vector $\boldsymbol{w}_o$ is expressed as [38]

$$\boldsymbol{w}_o = \boldsymbol{R}^{-1}\boldsymbol{\rho}, \tag{2.11}$$

where $\boldsymbol{R}$ is the autocorrelation matrix of the received vector $\boldsymbol{y}$ and $\boldsymbol{\rho}$ stands for the cross-correlation between $\boldsymbol{y}$ and $x$. A major drawback of this detector is inverting $\boldsymbol{R}$ which is of size $L$ and requires complexity of order $\mathcal{O}(L^3)$ [39]. As $L$ is usually large, the complexity will be very high. By imposing a constraint, and processing only $U$ out of $L$ relays the complexity could be reduced to order $\mathcal{O}(U^3)$, where $U \ll L$. Therefore, an efficient preprocessing matrix $\boldsymbol{P}$, is required which reduces $\boldsymbol{y}$ to $\bar{\boldsymbol{y}}$ or more formally

$$\bar{\boldsymbol{y}} = \boldsymbol{P}^H\boldsymbol{y}, \tag{2.12}$$

where $(\bar{\cdot})$ denotes a $U$-dimensional vector. Preprocessing matrix based on Krylov subspace has received a lot of interest in literature (see [12,17] and references therein). The main advantage of adopting the Krylov subspace method is that it is less complex than eigenvalue decomposition methods and the size of $U$ does not scale with $L$ [12]. The preprocessing matrix $\boldsymbol{P}$, of size $L \times U$, for the Krylov subspace method is given as

$$P = [h, Rh, \dots, R^{U-1}h]. \qquad (2.13)$$

From the above equation, it is observed that the preprocessing matrix requires complete knowledge of the CSI, the auto-correlation matrix $\boldsymbol{R}$, and $U$. With the Joint Iterative Optimization (JIO) algorithm, the preprocessing matrix $\boldsymbol{P}$ and the reduced weight vector $\bar{\boldsymbol{w}}$ are determined as follows [18]

$$\boldsymbol{P}(i+1) = \boldsymbol{P}(i) + \frac{\eta}{\|\boldsymbol{y}(i)\|^2 \|\bar{\boldsymbol{w}}(i)\|^2} e^*(i)\boldsymbol{y}(i)\bar{\boldsymbol{w}}^H(i), \qquad (2.14)$$

$$\bar{\boldsymbol{w}}(i+1) = \bar{\boldsymbol{w}}(i) + \frac{\mu}{\|\bar{\boldsymbol{y}}(i)\|^2} e^*(i)\bar{\boldsymbol{y}}(i), \qquad (2.15)$$

where $e(i) = x(i) - \bar{\boldsymbol{w}}^H(i)\bar{\boldsymbol{y}}(i)$ is the estimation error and $\mu$ and $\eta$ are the adaptation step-sizes, which satisfy $0 < \mu, \eta < 2$. It can be observed from (2.14) and (2.15) that the updated preprocessing matrix and the weight matrix only depend on the transmitted input $x$, the received output $\boldsymbol{y}$, the previous weights $\boldsymbol{w}$, and the preprocessing matrix $\boldsymbol{P}$. By carrying out training, the preprocessing matrix and weights can be updated. However, the major drawback of using JIO algorithm is that $U$ is fixed to the maximum that is allowed by the constraint, i.e., $U_{max}$ . It is possible that a lower U achieves a performance that is equivalent to what $U_{max}$ achieves albeit at a less complexity. Therefore, it is important to find the optimal $U_{opt}$ for each frame, so that equivalent MSE performance is achieved with lower complexity.

## 2.3 Proposed Threshold based Adaptive Detection

In this section, a new algorithm is proposed. The algorithm is able to achieve the same MSE performance as that of $U_{max}$ but at a lower computational complexity. This algorithm further trades the MSE by using a threshold $\delta$, which results in comparable MSE performance but much lower computational complexity. Let us look at the algorithm in detail. For each frame, the instantaneous MSE is different which results in a different $U_{opt}$ that is calculated as

$$U_{opt} = arg \min_{U} \underbrace{\left|x - \bar{\boldsymbol{w}}^H \boldsymbol{P}^H \boldsymbol{y}\right|^2}_{\text{MSE}_U}, U = 1, \ldots, U_{max}. \tag{2.16}$$

In order to evaluate the above equation, $\boldsymbol{P}$ and $\bar{\boldsymbol{w}}$ are calculated as shown in (2.14) and (2.15). Moreover, $\boldsymbol{y}$ is the received signal and $x$ is the training symbol known at the destination. By choosing the optimum $U_{opt}$ for each frame, the best possible MSE performance is ensured. This optimum $U_{opt} \leq U_{max}$ for each frame, will result in lower computations but equivalent MSE performance.

A threshold ($\delta : 0.0 \leq \delta \leq 1.0$) can now be picked a priori. $\delta$ denotes the tolerable difference in MSE performance between the optimal $U_{opt}$ and the lower $U$. Next, the detector searches sequentially starting with $U = 1$ for the lowest $U$ that satisfies the threshold $\delta$. This will trade-off MSE performance with computational savings. Formally the above can be written as

$$\begin{aligned} \min \quad & U \\ \text{s.t.} \quad & \frac{\text{MSE}_U}{\text{MSE}_{U_{opt}}} \leq 1 + \delta \\ & 1 \leq U \leq U_{opt}. \end{aligned} \tag{2.17}$$

One important factor to consider when using this algorithm is how much complexity is added to the system. Firstly, this algorithm only operates at the end of the training phase. Secondly, due to the inherent structure of $\boldsymbol{P}$ as shown in (2.13), the algorithm can be initially trained for $U_{max}$ in the training phase, then depending upon the selected $U$, the corresponding columns of $\boldsymbol{P}$ can be extracted. This will result in considerable savings, as different $\boldsymbol{P}$'s will not be required to be trained independently for different $U$'s. Finally, the computational complexity is measured in terms of the number of multiplications and additions required to detect a symbol [12]. As multiplications are more complex as compared to additions, the computational complexity is measured with the help of number of multiplications. The number of multiplications to detect a symbol is equivalent to $3LU + 3U + L$.

## 2.4 Simulation Results and Discussion

In this section, the performance of the proposed algorithms is validated by simulations. We assume that the number of relays $L = 10$, the constraint on $U_{max} = 4$, the channel gains follow the Rayleigh distribution, the noise is complex AWGN, and the transmitted symbols have unity power. The normalized doppler frequency is $f_d T_s = 10^{-4}$. The frame has a length of 1000 symbols.

Fig. 2.2 shows the effect of step-sizes on the MSE of the system at SNR = 0 dB. A total of $10^6$ independent realizations are carried out to obtain the ensemble average. The MSE of the ideal MMSE with complete CSI knowledge is also plotted as a benchmark. From the figure, it is observed that the convergence speed of the algorithm is dependent on the step-size. A bigger step-size converges faster, but to a higher MSE. On the contrary, the curve with a smaller step-size converges slower, but achieves lower MSE. From Fig. 2.2, it is observed that for a step-size of $\mu = \eta = 0.1$, the algorithm converges to the ideal MMSE with less than 250 training symbols. Therefore, the step-sizes are fixed to $\mu = \eta = 0.1$ and the training length is fixed to 250 training

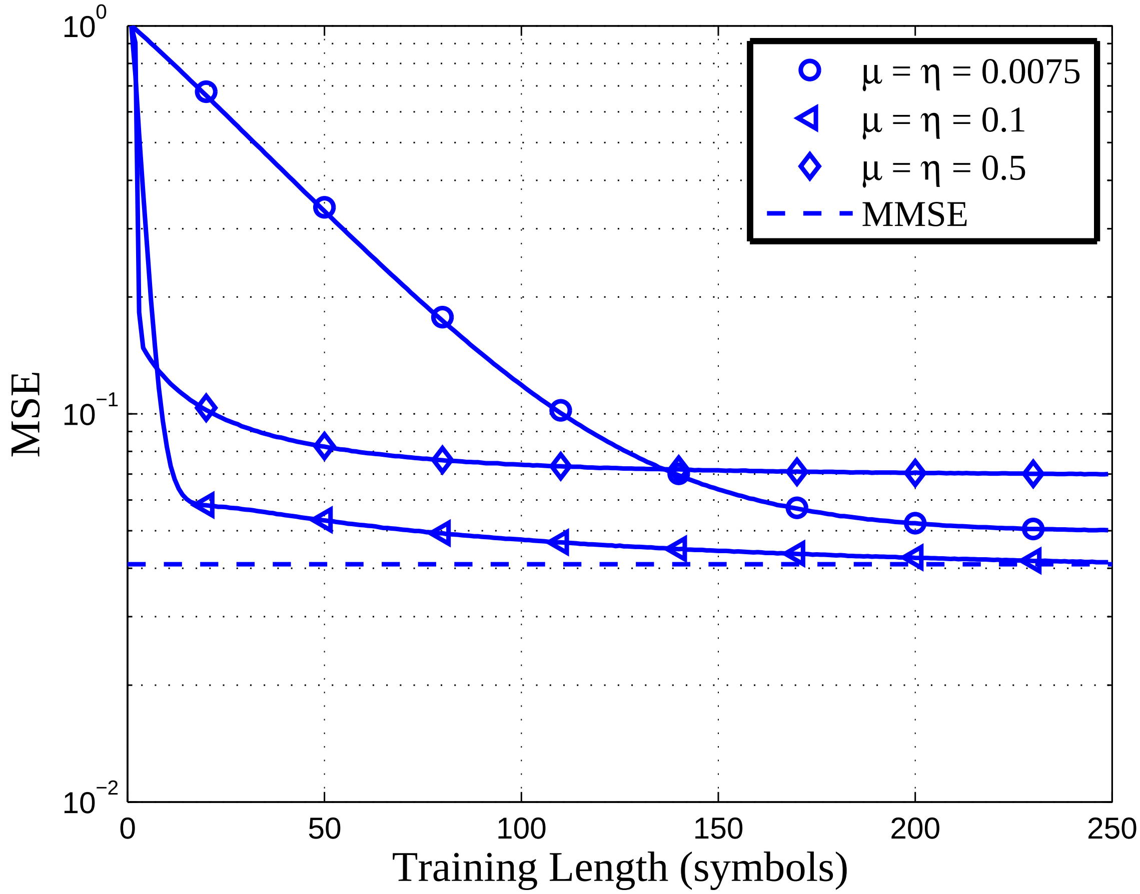


Figure 2.2: Learning curves when communicating with different step-sizes. The parameters are SNR $= 0$ dB, normalized doppler frequency $f_d T_s = 10^{-4}$, $L = 10$, and $U_{max} = 4$.

symbols.

Fig. 2.3 compares the SNR versus BER performance of our proposed algorithms with that of the JIO algorithm. The JIO algorithm is employed with $U = U_{max} = 4$. From the simulation, it is observed that when $\sigma^2_{\epsilon_g} = \sigma^2_{\epsilon_h} = 0.0$, the proposed algorithm achieves the same BER performance as that of the JIO with $U_{avg} = 3.34$ when $\delta = 0\%$. By increasing the threshold $\delta$ by 5% and 10%, the MSE is relaxed and the average $U$ decreases to $U_{avg} = 2.23$ and $U_{avg} = 1.68$, respectively. Relaxing the MSE results in designing a processing matrix $\boldsymbol{P}$ with a lower $U$ which satisfies $\text{MSE}_U$ as stated in (2.17). The BER performance of the algorithm with $\delta = 5\%$ and $\delta = 10\%$ is less

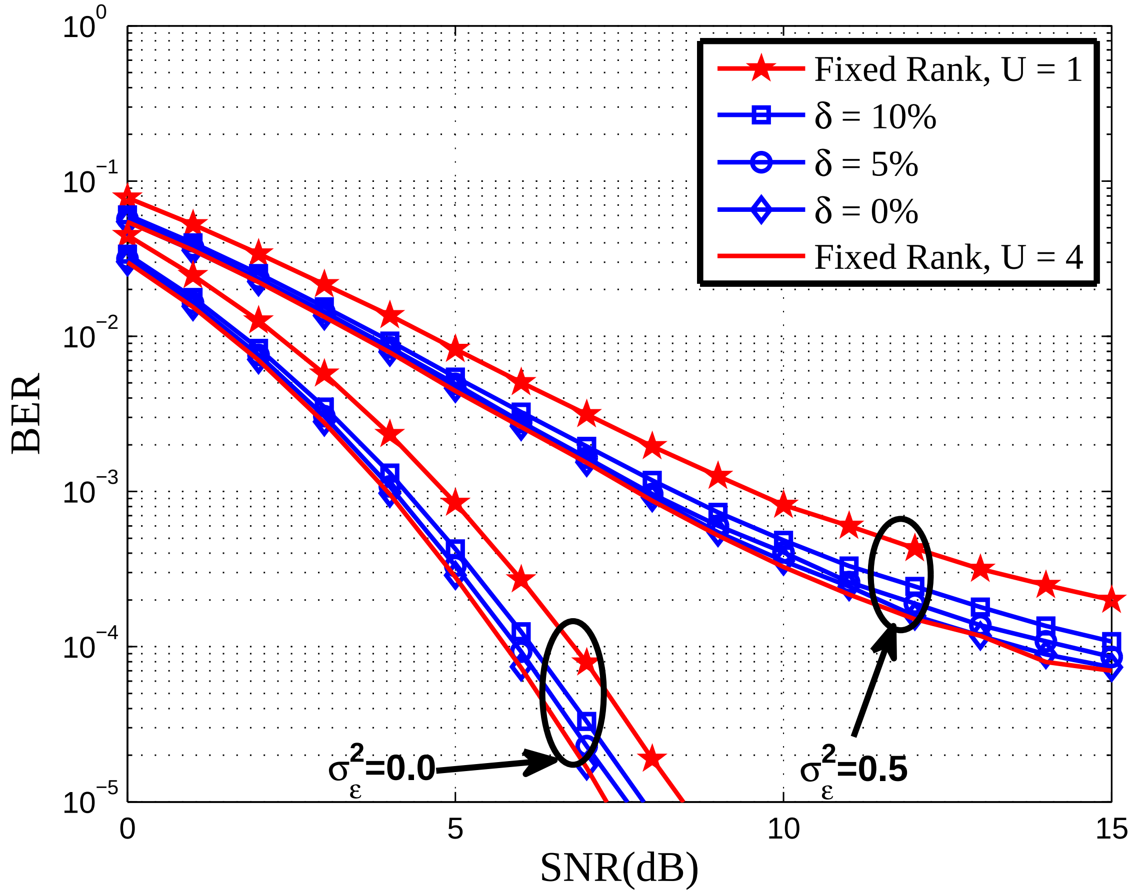


Figure 2.3: SNR versus BER performance of the proposed algorithm. The parameters are normalized doppler frequency $f_d T_s = 10^{-4}$, $L = 10$, and $U_{max} = 4$.

than half a dB away from the optimal performance achieved by the JIO algorithm. For the case where we have an estimation error, say, $\sigma^2_{\epsilon_g} = \sigma^2_{\epsilon_h} = 0.5$, the proposed algorithm achieves $U_{avg} = 3.51$ when $\delta = 0\%$. By increasing the threshold $\delta$ to 5% and 10%, the average $U$ decreases to $U_{avg} = 2.32$ and $U_{avg} = 1.79$, respectively. From the values just mentioned, it can be seen that a higher $U_{avg}$ is needed when there is an estimation error for each respective threshold $\delta$. It is worth mentioning that for $U = 1$, the JIO is equivalent to maximal ratio combiner (MRC). It has already been proved in [12] that $U = 1$ does not achieve the same BER performance as all participating relays when relays employ variable gain amplification.

Fig. 2.4 shows the percentage of computational complexity saved versus the percentage of performance lost at SNR = 6 dB. JIO with $U_{max} = 4$ set as the benchmark. The performance loss is calculated as the relative difference in BER achieved by our proposed algorithm compared to the BER achieved by the JIO algorithm. Computational saving is calculated as the relative difference between computations required by the proposed algorithm compared to the computations required by the JIO algorithm. In this figure, the variance of channel estimation is set to zero, making the assumption that the estimated channel is always equivalent to the exact channel. From Fig. 2.4, it can be observed that a reduction of more than 15% is achieved in terms of complexity when deploying our algorithm as compared with JIO with the same BER performance for $\delta = 0\%$. Furthermore, it can be observed that more than 25%, 50% and 60% in terms of complexity is saved when $\delta$ is relaxed by 2%, 10% and 20%, respectively.

Fig. 2.5 shows the percentage of computational complexity saved versus the percentage of performance lost also at SNR = 6 dB. JIO with $U_{max} = 4$ is set as a benchmark. The performance lost and computational saving are calculated as described in Fig. 2.4. It can be observed that a reduction of more than 10% is achieved in terms of complexity when deploying our algorithm as compared with JIO with the same BER performance for $\delta = 0\%$. Furthermore, it can be observed that around 40%, 50% and 60% in terms of complexity is saved when $\delta$ is relaxed by 5%, 10% and 20%, respectively.

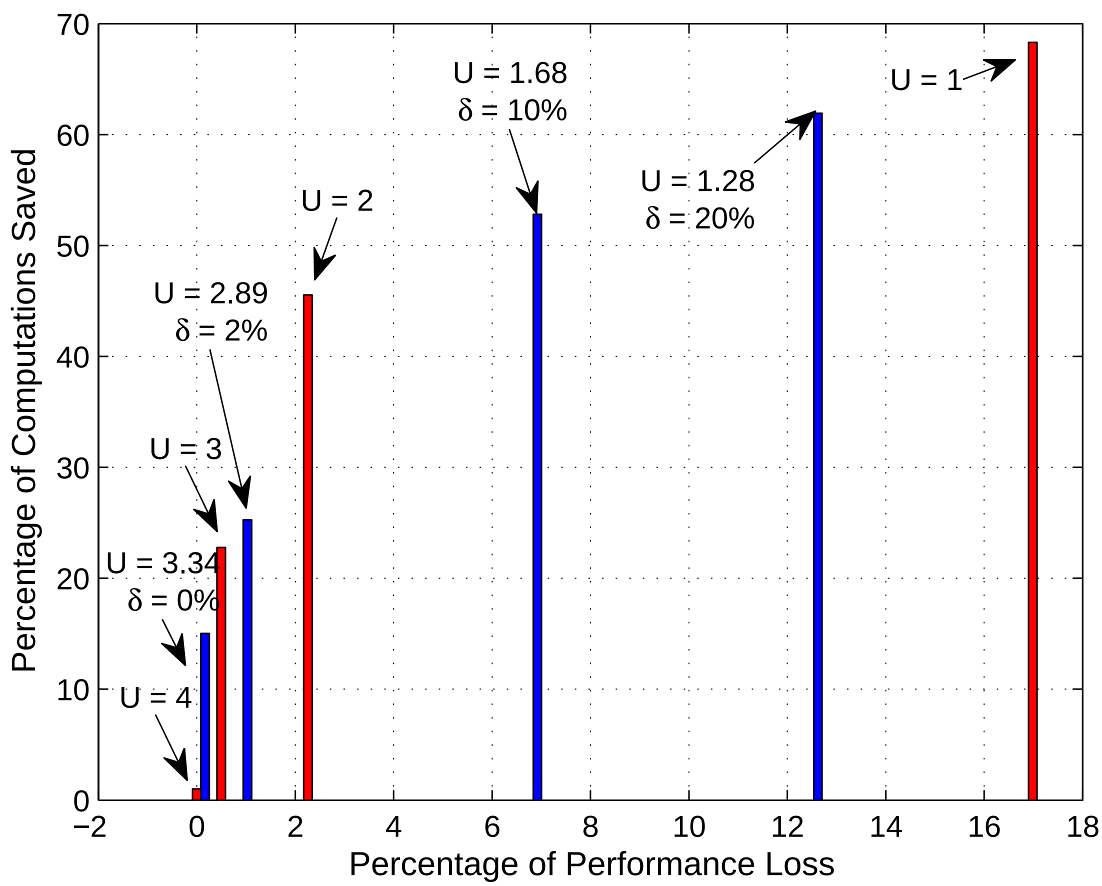


Figure 2.4: Percentage of performance loss versus computations saved. The parameters are SNR = 6 dB, normalized doppler frequency $f_d T_s = 10^{-4}$, $L = 10$ and $\sigma^2_{\epsilon_g} = \sigma^2_{\epsilon_h} = 0.0$.

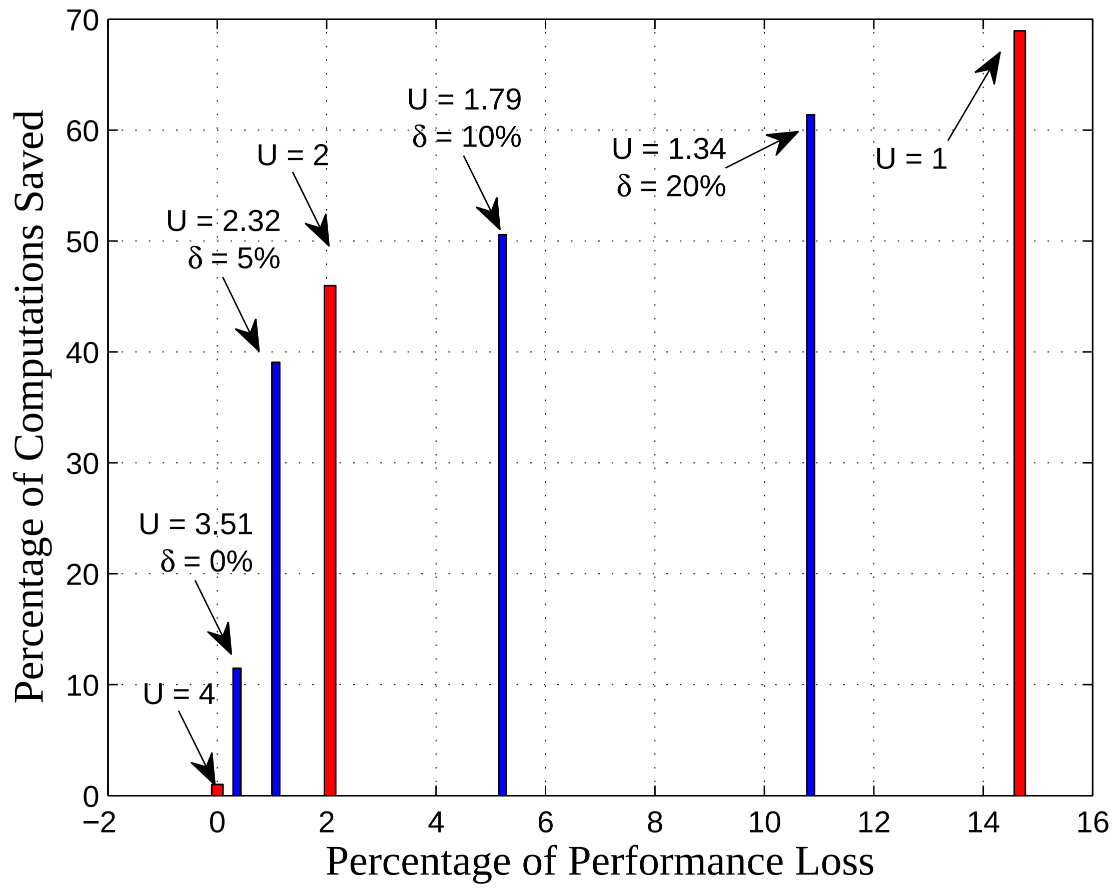


Figure 2.5: Percentage of performance loss versus computations saved. The parameters are SNR = 6 dB, normalized doppler frequency $f_d T_s = 10^{-4}$, $L = 10$, and $\sigma^2_{\epsilon_g} = \sigma^2_{\epsilon_h} = 0.5$.

# Chapter 3

# Adaptive Detector Based on Minimum Symbol Error Rate Criteria

In this chapter, we design a joint preprocessor-based MSER detector (JP-MSER) for systems that have limited training length available. In addition, we design a new preprocessor matrix based on minimizing the SER for the detector. Similar performance as the ML detector is achieved by using our proposed detector with a lower computational complexity. Finally, we assume that perfect channel knowledge is unavailable at the receiver side.

## 3.1 System Model

### 3.1.1 One-Way Relaying

The cooperative network considered in this part is shown in Fig. 3.1, which is the same system model adopted in [11, 27, 31, 34]. It is also similar to the system in Chapter 2, but we will include it here for completeness. The source $S$ transmits its information data to the destination $D$ with the help of $L$ relays denoted by $R_l$ where

$l = 1, 2, \ldots, L$. The transmission happens in two phases. In phase I, the source broadcasts the information to the $L$ relays, while in phase II the relays amplify then forward the data to the destination. Due to the large distance, there is no direct link between S and D. The channel between the source and the $l$th relay is denoted by $h_{SR_l}$ with variance $\sigma^2_{h_{SR_l}}$, while the channel between the the $l$th relay and the destination is denoted by $h_{R_lD}$ with variance $\sigma^2_{h_{R_lD}}$. In order to mitigate interference and treat the channel as a single tap, orthogonality can be used in either frequency or time domain [27]. The received signal is represented as

$$\boldsymbol{y} = \boldsymbol{h}x + \boldsymbol{n}, \tag{3.1}$$

where $x$ is the broadcasted symbol by $S$ with variance of $\sigma_x^2 = \mathbf{E}[xx^*] = 1$. The channel and the noise vectors are given as

$$\boldsymbol{h} = \begin{bmatrix} \zeta_{R_1} h_{SR_1} h_{DR_1} \\ \vdots \\ \zeta_{R_L} h_{SR_L} h_{DR_L}, \end{bmatrix}, \quad \boldsymbol{n} = \begin{bmatrix} \zeta_{R_1} h_{DR_1} n_{R_1} + n_{D_1} \\ \vdots \\ \zeta_{R_L} h_{DR_L} n_{R_L} + n_{D_L} \end{bmatrix}, \tag{3.2}$$

where $1/\zeta_{R_l} = \sqrt{|h_{SR_l}|^2 + \sigma^2_{R_l}}$ is the variable amplification factor at the $l$th relay [36]. Finally, The covariance of noise is given as $\boldsymbol{\Sigma} = E[\boldsymbol{n}\boldsymbol{n}^H]$.

### 3.1.2 Two-Way Relaying

The cooperative network considered in this part is shown in Fig. 3.2 [40]. The two sources $S$ and $D$ transmit their symbols to each other with the help of $L$ relays denoted by $R_l$ where $l = 1, 2, \ldots, L$. The transmission happens in two phases. In phase I, the two sources broadcast the information to the $L$ relays, while in phase II each relay combines its data and retransmits it in both directions. A direct link between the source and destination is ignored due to the large distance between $S$

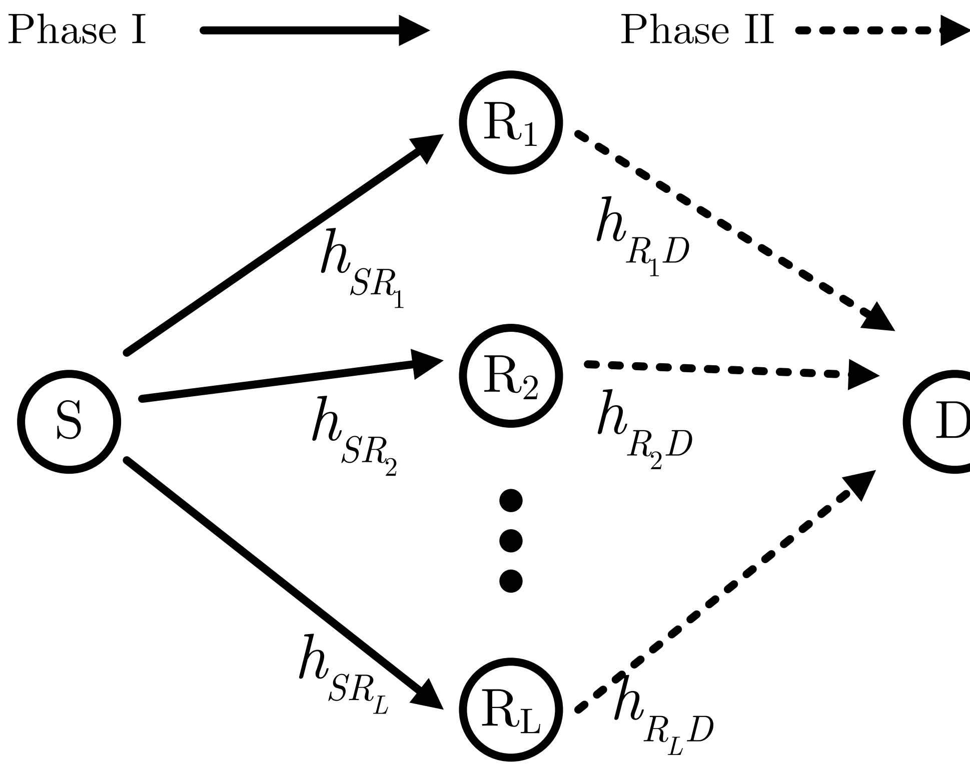


Figure 3.1: Block diagram of a one-way cooperative communication network with $L$ relays.

and $D$. The channel is not assumed to be reciprocal, meaning that the channel from $S$ to $R_l$ is different from the channel from $R_l$ to $S$. The channel from $S$ to the $l$th relay is denoted by $h_{SR_l}$ with variance $\sigma^2_{h_{SR_l}}$, while the channel from the $l$th relay to $D$ is denoted by $h_{R_lD}$ with variance $\sigma^2_{h_{R_lD}}$. Similarly, in the reverse direction, the channel from $D$ to the $l$th relay is denoted by $h_{DR_l}$ with variance $\sigma^2_{h_{DR_l}}$, while the channel from the $l$th relay to $S$ is denoted by $h_{R_lS}$ with variance $\sigma^2_{h_{R_lS}}$. In order to mitigate interference and treat the channel as a single tap, orthogonality can be used in either frequency or time domain [27]. The symbols $x_1$ broadcasted by $S$ and $x_2$ broadcasted by $D$ are received at the $l$th relay as

$$y_{R_l} = h_{SR_l}x_1 + h_{DR_l}x_2 + n_{R_l}, \quad l = 1, 2, \ldots, L, \tag{3.3}$$

where $x_1$ and $x_2$ have average energy of $\sigma_x^2 = \mathbf{E}[xx^*] = 1$, and $n_{R_l}$ denotes the complex additive white Gaussian noise (AWGN) added at the $l$th relay with zero mean and variance $\sigma_{R_l}^2$, i.e., depending upon the channel gains, each relay might have a different variance.

In phase II, each relay amplifies its signal with an amplification factor $\zeta_{R_l}$ that works to normalize the power transmitted from the relays and is given as

$$\zeta_{R_l} = \sqrt{\frac{1}{|h_{SR_l}|^2 + |h_{DR_l}|^2 + \sigma_{R_l}^2}}, \quad l = 1, 2, \ldots, L. \tag{3.4}$$

We will consider the signal received by $D$, but one can equally consider the other direction since it is symmetric. $\zeta_{R_l} y_{R_l}$, which is the new symbol to be transmitted by the relays to the destination, can be written as

$$\begin{aligned} y_l &= h_{R_l D}\zeta_{R_l} y_{R_l} + n_{D_l}, \quad l = 1, 2, \ldots, L, \\ &= \zeta_{R_l} h_{R_l D} h_{SR_l} x_1 + \zeta_{R_l} h_{R_l D} h_{DR_l} x_2 \\ &+ \zeta_{R_l} h_{R_l D} n_{R_l} + n_{D_l}, \quad l = 1, 2, \ldots, L, \end{aligned} \tag{3.5}$$

where $n_{D_l}$ is complex AWGN noise with zero mean and variance $\sigma_D^2$. Finally, (3.5) is written in vector form as

$$\boldsymbol{y} = \boldsymbol{h}_1 x_1 + \boldsymbol{h}_2 x_2 + \boldsymbol{n}. \tag{3.6}$$

The channel and the noise vectors are given as

$$\boldsymbol{h}_1 = \begin{bmatrix} \zeta_{R_1} h_{R_1 D} h_{SR_1} \\ \vdots \\ \zeta_{R_L} h_{R_L D} h_{SR_L}, \end{bmatrix}, \quad \boldsymbol{h}_2 = \begin{bmatrix} \zeta_{R_1} h_{R_1 D} h_{DR_1} \\ \vdots \\ \zeta_{R_L} h_{R_L D} h_{DR_L}, \end{bmatrix},$$
$$\boldsymbol{n} = \begin{bmatrix} \zeta_{R_1} h_{R_1 D} n_{R_1} + n_{D_1} \\ \vdots \\ \zeta_{R_L} h_{R_L D} n_{R_L} + n_{D_L} \end{bmatrix}. \tag{3.7}$$

Since this is a two-way relaying system, $x_2$ is always known to $D$, so after the estimation of $h_2$ we can cancel the self-interference and get

$$\boldsymbol{y} = \boldsymbol{h}_1 x_1 + \boldsymbol{n}, \tag{3.8}$$

where the covariance of noise is given as $\boldsymbol{\Sigma} = E[\boldsymbol{n}\boldsymbol{n}^H]$. As can be seen, two-way is similar to the one-way relying scenario with the exception of the amplification factor, and hence, the detection for both cases will be quite similar as shown in the next section.

## 3.2 Detection for the Cooperative Networks

As we want our weight vector to process $U$ out of $L$ signals, an efficient preprocessing matrix $\boldsymbol{P}$ is required, which reduces the system from size $L$ to $U$.

$$\bar{\boldsymbol{y}} = \boldsymbol{P}^H \boldsymbol{y}, \tag{3.9}$$

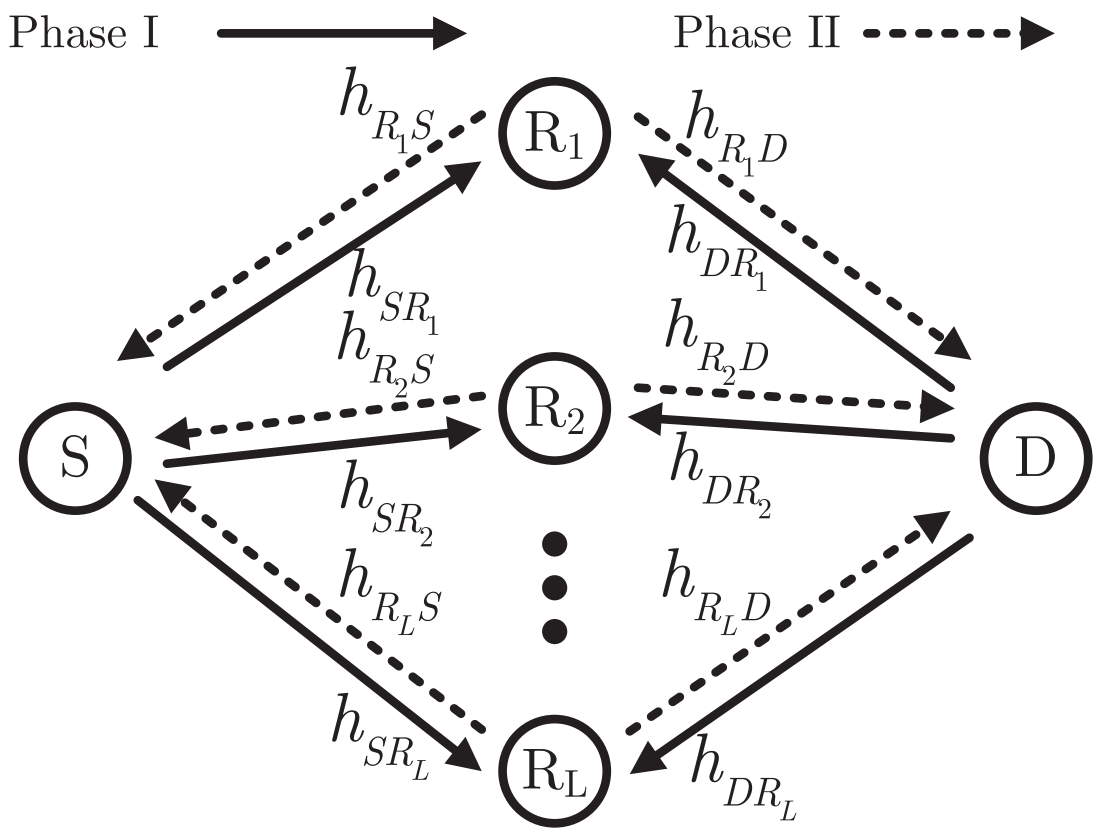


Figure 3.2: Block diagram of a two-way cooperative communication network with $L$ relays.

where $\bar{(\cdot)}$ denotes a $U$-dimensional vector. $\boldsymbol{P} = [\boldsymbol{p}_1, \ldots, \boldsymbol{p}_U]$ and $\boldsymbol{p}_u$ is the u-$th$ complex vector of size $L$. After linear filtering the output of the $z$ is given as

$$\begin{aligned} z &= \bar{\boldsymbol{w}}^H \bar{\boldsymbol{y}} = \bar{\boldsymbol{w}}^H \boldsymbol{P}^H \boldsymbol{y} \\ &= \bar{\boldsymbol{w}}^H \boldsymbol{P}^H \boldsymbol{h} x + \bar{\boldsymbol{w}}^H \boldsymbol{P}^H \boldsymbol{n}, \end{aligned} \tag{3.10}$$

where $\bar{\boldsymbol{w}} = [w_1, \ldots, w_U]^T$ and $w_u$ is the u-$th$ tap filter complex coefficient. The estimate of the symbol $x$ can be written as

$$\begin{aligned}
\hat{x} &= sgn(z_R) + jsgn(z_I) \\
&= sgn(\Re(\bar{\boldsymbol{w}}^H \boldsymbol{P}^H \boldsymbol{h} x) + \Re(\bar{\boldsymbol{w}}^H \boldsymbol{P}^H \boldsymbol{n})) \\
&+ jsgn(\Im(\bar{\boldsymbol{w}}^H \boldsymbol{P}^H \boldsymbol{h} x) + \Im(\bar{\boldsymbol{w}}^H \boldsymbol{P}^H \boldsymbol{n})),
\end{aligned} \tag{3.11}$$

where $z_R = \Re(z)$ and $z_I = \Im(z)$ are the real and imaginary parts, respectively. To find the probability density function (PDF) of the noise, and assuming that $\boldsymbol{n}$ is Gaussian, then $\bar{\boldsymbol{w}}^H \boldsymbol{P}^H \boldsymbol{n}$ is also Gaussian since it is merely a linear combination of $\boldsymbol{n}$. The variance in that case will be $\bar{\boldsymbol{w}}^H \boldsymbol{P}^H \boldsymbol{\Sigma} \boldsymbol{P} \bar{\boldsymbol{w}}/2$. Assuming independence between the real and imaginary parts, the probability density function (PDF) of $z_R$ and $z_I$ can be written as

$$p_{z_R|x} = \frac{1}{\sqrt{\pi \bar{\boldsymbol{w}}^H \boldsymbol{P}^H \boldsymbol{\Sigma} \boldsymbol{P} \bar{\boldsymbol{w}}}} \exp\left(-\frac{(z_R - \Re(\bar{\boldsymbol{w}}^H \boldsymbol{P}^H \boldsymbol{h} x))^2}{\bar{\boldsymbol{w}}^H \boldsymbol{P}^H \boldsymbol{\Sigma} \boldsymbol{P} \bar{\boldsymbol{w}}}\right), \tag{3.12}$$

$$p_{z_I|x} = \frac{1}{\sqrt{\pi \bar{\boldsymbol{w}}^H \boldsymbol{P}^H \boldsymbol{\Sigma} \boldsymbol{P} \bar{\boldsymbol{w}}}} \exp\left(-\frac{(z_I - \Im(\bar{\boldsymbol{w}}^H \boldsymbol{P}^H \boldsymbol{h} x))^2}{\bar{\boldsymbol{w}}^H \boldsymbol{P}^H \boldsymbol{\Sigma} \boldsymbol{P} \bar{\boldsymbol{w}}}\right), \tag{3.13}$$

where $\Re(\bar{\boldsymbol{w}}^H \boldsymbol{P}^H \boldsymbol{h} x)$ and $\Im(\bar{\boldsymbol{w}}^H \boldsymbol{P}^H \boldsymbol{h} x)$ are the respective means of $z_R$ and $z_I$. For complex modulation, $x = a + jb$, the probability of correct symbol detection is $P_c = (1 - P_{a,e})(1 - P_{b,e}) = 1 - P_{a,e} - P_{b,e} + P_{a,e}P_{b,e}$, and the error probability is $P_e = 1 - P_c = P_{a,e} + P_{b,e} - P_{a,e}P_{b,e}$. Assuming the term $P_{a,e}P_{b,e}$ is small with respect to

$P_{a,e}$ and $P_{a,e}$, the probability of error for QPSK symbols is derived as follows

$$\begin{aligned} P_e(\bar{\boldsymbol{w}},\ \boldsymbol{P}) &= \int_{-\infty}^{0} P(z_R|x_R=+1)P(x_R=+1)dz_R \\ &+ \int_{0}^{\infty} P(z_R|x_R=-1)P(x_R=-1)dz_R \\ &+ \int_{-\infty}^{0} P(z_I|x_I=+1)P(x_I=+1)dz_I \\ &+ \int_{0}^{\infty} P(z_I|x_I=-1)P(x_I=-1)dz_I. \end{aligned} \tag{3.14}$$

For equally likely symbols, this can be simplified to

$$\begin{aligned} P_e(\bar{\boldsymbol{w}},\boldsymbol{P}) &= \int_{-\infty}^{0} P(z_R|x_R=+1)dz_R + \int_{-\infty}^{0} P(z_I|x_I=+1)dz_I \\ &= \int_{-\infty}^{0} \frac{\exp\left(-\frac{(z_R-\Re(\bar{\boldsymbol{w}}^H\boldsymbol{P}^H\boldsymbol{h}))^2}{\bar{\boldsymbol{w}}^H\boldsymbol{P}^H\boldsymbol{\Sigma}\boldsymbol{P}\bar{\boldsymbol{w}}}\right)}{\sqrt{\pi\bar{\boldsymbol{w}}^H\boldsymbol{P}^H\boldsymbol{\Sigma}\boldsymbol{P}\bar{\boldsymbol{w}}}}dz_R + \int_{-\infty}^{0} \frac{\exp\left(-\frac{(z_I-\Im(\bar{\boldsymbol{w}}^H\boldsymbol{P}^H\boldsymbol{h}))^2}{\bar{\boldsymbol{w}}^H\boldsymbol{P}^H\boldsymbol{\Sigma}\boldsymbol{P}\bar{\boldsymbol{w}}}\right)}{\sqrt{\pi\bar{\boldsymbol{w}}^H\boldsymbol{P}^H\boldsymbol{\Sigma}\boldsymbol{P}\bar{\boldsymbol{w}}}}dz_I \\ &= Q\left(\frac{\sqrt{2}\Re(\bar{\boldsymbol{w}}^H\boldsymbol{P}^H\boldsymbol{h})}{\sqrt{\bar{\boldsymbol{w}}^H\boldsymbol{P}^H\boldsymbol{\Sigma}\boldsymbol{P}\bar{\boldsymbol{w}}}}\right) + Q\left(\frac{\sqrt{2}\Im(\bar{\boldsymbol{w}}^H\boldsymbol{P}^H\boldsymbol{h})}{\sqrt{\bar{\boldsymbol{w}}^H\boldsymbol{P}^H\boldsymbol{\Sigma}\boldsymbol{P}\bar{\boldsymbol{w}}}}\right), \end{aligned} \tag{3.15}$$

where $Q(\cdot)$ is the standard Gaussian Q-function, defined as [41]

$$Q(u) = \frac{1}{\sqrt{2\pi}} \int_{u}^{\infty} \exp\left(-\frac{v^2}{2}\right) dv. \tag{3.16}$$

From (3.15), it can be observed that in order to minimize the probability of error, designing suitable $\bar{\boldsymbol{w}}$ and $\boldsymbol{P}$ is important. To the best of our knowledge, most of the existing literature minimized the mean square error (MSE), where $\boldsymbol{P}$ is designed by a MSWF and $\boldsymbol{w}$ is equivalent to the weights of the MMSE detector [11, 27].

### 3.2.1 JP-MSER Algorithm

With such a probability of error, the weights and the preprocessing matrix will not have a closed-form solution and an iterative algorithm is required to obtain the solution. Using the steepest descent (SD) algorithm, the weights and the preprocessing matrix can be determined. The following steps are carried out.

**Step 1:** Initialize the weights of the filter and the preprocessing matrix randomly with the conditions: $\bar{\boldsymbol{w}}^H \bar{\boldsymbol{w}} = 1/E_b$ and $tr(\boldsymbol{P}^H \boldsymbol{P}) = 1/E_b$, where $E_b$ is the bit energy and depends upon the modulation.

**Step 2:** As exact channel knowledge is not available, $\boldsymbol{h}$ is estimated as follows in the case of one-way relaying

$$\hat{\boldsymbol{h}}(i) = \frac{i\hat{\boldsymbol{h}}(i-1) + \frac{\boldsymbol{y}(i)}{x(i)}}{i+1}, \tag{3.17}$$

while in the case of two-way relaying the estimation equations change to

$$\hat{\boldsymbol{h}}_1(i) = \frac{i\hat{\boldsymbol{h}}_{\mathbf{1}}(i-1) + \frac{\boldsymbol{y}(i) - \hat{\boldsymbol{h}}_2(i-1)x_2(i)}{x_1(i)}}{i+1}, \tag{3.18}$$

$$\hat{\boldsymbol{h}}_2(i) = \frac{i\hat{\boldsymbol{h}}_{\mathbf{2}}(i-1) + \frac{\boldsymbol{y}(i) - \hat{\boldsymbol{h}}_1(i-1)x_1(i)}{x_2(i)}}{i+1}, \tag{3.19}$$

where $\hat{\boldsymbol{h}}(-1) = \hat{\boldsymbol{h}}_{\mathbf{1}}(-1) = \hat{\boldsymbol{h}}_{\mathbf{2}}(-1) = \mathbf{0}$, and $i$ represents the index of iteration.

**Step 3:** Because of imperfect channel knowledge the covariance matrix $\boldsymbol{\Sigma}$ also needs to be estimated. The estimated covariance matrix in the one-way case is given as

$$\hat{\boldsymbol{\Sigma}}(i) = \frac{i\hat{\boldsymbol{\Sigma}}(i-1) + \left(\boldsymbol{y}(i) - \hat{\boldsymbol{h}}(i)x(i)\right)\left(\boldsymbol{y}(i) - \hat{\boldsymbol{h}}(i)x(i)\right)^H}{i+1}, \tag{3.20}$$

while in the two-way case it is altered as follows

$$\hat{\boldsymbol{n}}(i) = \boldsymbol{y}(i) - \hat{\boldsymbol{h}}_1(i)x_1(i) - \hat{\boldsymbol{h}}_2(i)x_2(i), \tag{3.21}$$

$$\hat{\boldsymbol{\Sigma}}(i) = \frac{i\hat{\boldsymbol{\Sigma}}(i-1) + \hat{\boldsymbol{n}}(i)\hat{\boldsymbol{n}}^H(i)}{i+1}, \tag{3.22}$$

where the covariance matrix is initialized by $\hat{\boldsymbol{\Sigma}}(-1) = \mathbf{0}$.

**Step 4:** Determine the gradients of $P_e(\bar{\boldsymbol{w}},\ \boldsymbol{P})$ with respect to $\bar{\boldsymbol{w}}$ and $\boldsymbol{P}$ using (3.25) and (3.26), respectively. To simplify the gradients, we assume that $a = \bar{\boldsymbol{w}}^H\boldsymbol{P}^H\hat{\boldsymbol{\Sigma}}\boldsymbol{P}\bar{\boldsymbol{w}}$, and $b = \bar{\boldsymbol{w}}^H\boldsymbol{P}^H\hat{\boldsymbol{h}}$.

**Step 5:** Update $\bar{\boldsymbol{w}}$ and $\boldsymbol{P}$ using the following formulas:

$$\bar{\boldsymbol{w}}(i+1) = \bar{\boldsymbol{w}}(i) - \mu\nabla_{\bar{\boldsymbol{w}}}P_e(\bar{\boldsymbol{w}}(i),\ \boldsymbol{P}(i)), \tag{3.23}$$

$$\boldsymbol{P}(i+1) = \boldsymbol{P}(i) - \eta\nabla_{\boldsymbol{P}}P_e(\bar{\boldsymbol{w}}(i),\ \boldsymbol{P}(i)), \tag{3.24}$$

where $\mu$ and $\eta$ are the suitable learning rates.

**Step 6:** After each iteration, normalize in order to have $\bar{\boldsymbol{w}}^H\bar{\boldsymbol{w}} = 1/E_b$ and $tr(\boldsymbol{P}^H\boldsymbol{P}) = 1/E_b$.

---

$$\begin{aligned}\nabla_{\bar{\boldsymbol{w}}}P_e(\bar{\boldsymbol{w}},\ \boldsymbol{P}) &= \frac{1}{\sqrt{\pi}}\frac{\Re(b)\boldsymbol{P}^H\hat{\boldsymbol{\Sigma}}\boldsymbol{P}\bar{\boldsymbol{w}} - a\boldsymbol{P}^H\hat{\boldsymbol{h}}}{a^{\frac{3}{2}}}\exp\left(-\frac{\Re(b)^2}{a}\right)\\ &+\frac{1}{\sqrt{\pi}}\frac{\Im(b)\boldsymbol{P}^H\hat{\boldsymbol{\Sigma}}\boldsymbol{P}\bar{\boldsymbol{w}} + ja\boldsymbol{P}^H\hat{\boldsymbol{h}}}{a^{\frac{3}{2}}}\exp\left(-\frac{\Im(b)^2}{a}\right)\end{aligned} \tag{3.25}$$

$$\begin{aligned}\nabla_{\boldsymbol{P}}P_e(\bar{\boldsymbol{w}},\ \boldsymbol{P}) &= \frac{1}{\sqrt{\pi}}\frac{\Re(b)\hat{\boldsymbol{\Sigma}}\boldsymbol{P}\bar{\boldsymbol{w}}\bar{\boldsymbol{w}}^H - a\hat{\boldsymbol{h}}\bar{\boldsymbol{w}}^H}{a^{\frac{3}{2}}}\exp\left(-\frac{\Re(b)^2}{a}\right)\\ &+\frac{1}{\sqrt{\pi}}\frac{\Im(b)\hat{\boldsymbol{\Sigma}}\boldsymbol{P}\bar{\boldsymbol{w}}\bar{\boldsymbol{w}}^H + ja\hat{\boldsymbol{h}}\bar{\boldsymbol{w}}^H}{a^{\frac{3}{2}}}\exp\left(-\frac{\Im(b)^2}{a}\right)\end{aligned} \tag{3.26}$$

### 3.2.2 Computational Complexity

The computational complexity of these update equations seems high, but a good analysis shows that the order of complexity is $\mathcal{O}(L^2)$. When the noise in independent and $\Sigma$ is diagonal then the complexity reduces to $\mathcal{O}(LU)$. Note also that $U$ in this MSER detector is as low as 1 reducing the order of complexity to $\mathcal{O}(L)$ most of the time. The update equations in (3.25) and (3.26) might seem complicated but there are a lot of reused expressions; for example, it is enough to compute $\bar{\boldsymbol{w}}^H \boldsymbol{P}^H \boldsymbol{\Sigma} \boldsymbol{P} \bar{\boldsymbol{w}}$ once for every iteration and reuse it 12 times in the update equations.

Table 3.1: Computational Complexity.

| Algorithms | Number of Multiplications |
|---|---|
| ML | $L^3/3 + 4L^2 + 4L$ |
| CS-based MMSE | $L^3 + 3L^2 + 2U^2 + U^3/3 + UL^2 + U^2L + U$ |
| TPA-based MMSE | $U^3/3 + UL^2 + U^2L + (U-1)L^2 + 2LU + U$ |
| JP-MSER | $L^2 + 10LU + 7U$ |

## 3.3 Simulation Results and Discussion

The BER performance of the cooperative system is discussed in this section. We start with the results of one-way relaying and then we move on to two-way relaying. A channel with Rayleigh distribution is assumed. We consider a communication channel with quasi-static nature where the channel is assumed to be constant during a block of symbols and take an independent value for the next block. The size of the system $L$ is chosen to be 10. The number of iterations is fixed to 400, although the algorithm converges well for as low as 200 iterations. The transmitted symbol has unity power and the variance each channel is unity. Finally, the symbols are using QPSK modulation.

In Fig. 3.3, the effect of learning rates on the BER of the one-way system is shown

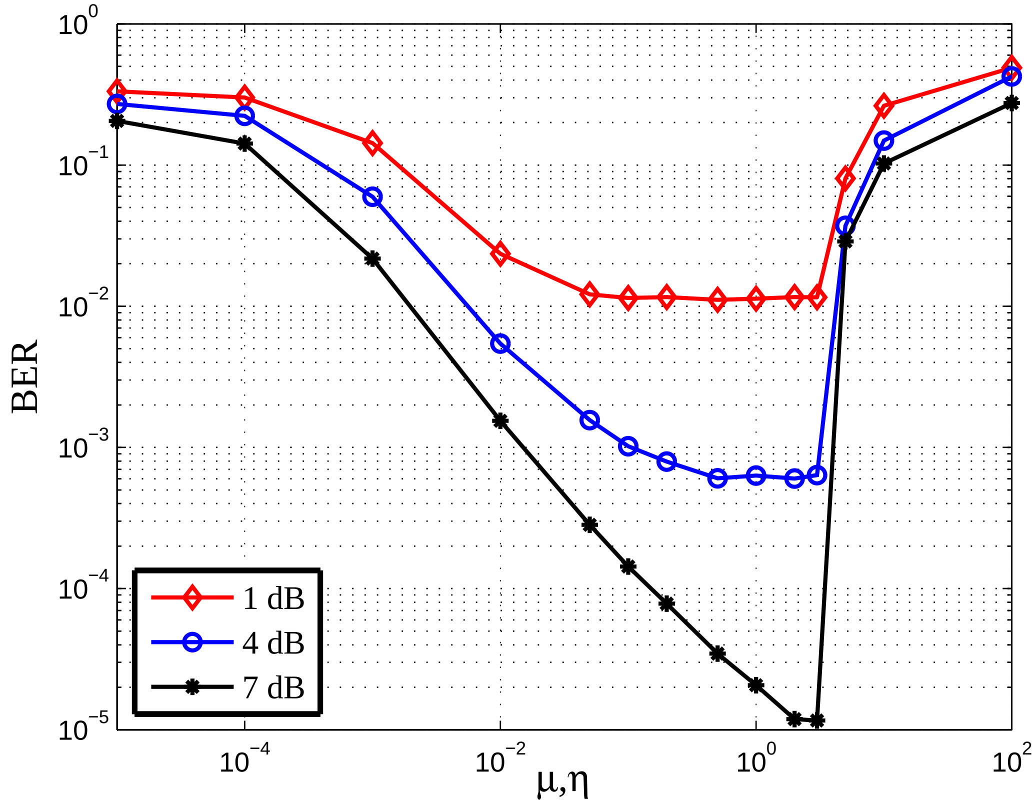


Figure 3.3: The BER of the one-way relaying system versus the step-size.

at three SNR values. The simulation carried out 3000 independent realizations of the channel. From the figure, it is observed that the convergence speed of the algorithm is dependent on the step-size. The convergence achieved after 400 iterations is showed for a range of step sizes. In the simulation, $\mu$ and $\eta$ are fixed to the same value for simplicity. From Fig. 3.3, it can be observed that a learning rate of $1 < \mu, \eta < 3$ gives excellent performance across all SNR values, while a smaller step-size than 1 converges slowly and hence will need more than 400 iterations. Therefore, in the detection phase, the learning rates are fixed to $\mu = 3$ and $\eta = 3$ for the one-way system.

Fig. 3.4 compares the SNR versus BER performance of a range of detectors with the optimal ML detector. Starting with the CS detector, a drastic loss in performance is evident when $U = 1$, however the diversity order will be same as all participating

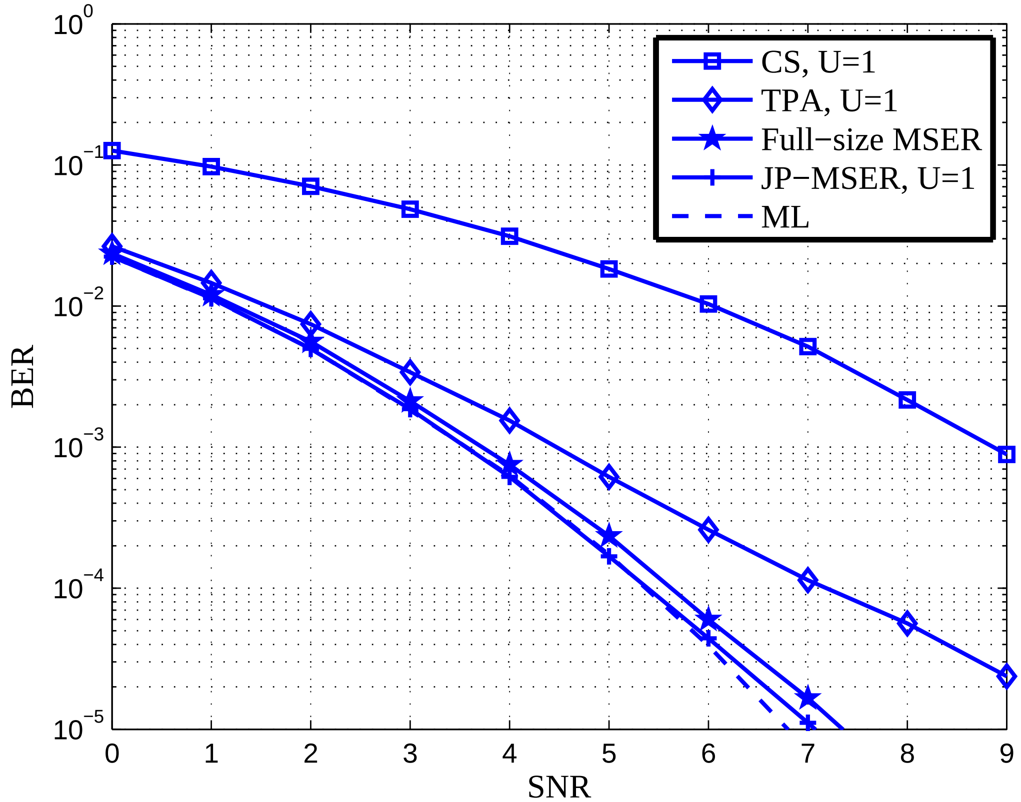


Figure 3.4: BER vs. SNR performance for the proposed one-way detector contrasted with other detectors in the literature.

relays. Next, the performance of the TPA-based MMSE detector is shown, again, with $U = 1$. It is worth mentioning here that for $U = 1$, TPA-based MMSE detector is equivalent to maximal ratio combiner (MRC) and a loss of $1.5dB$ is observed for a BER of $10^{-4}$. Finally, the results of our proposed detector is shown. The full-rank MSER detector which utilizes all participating relays is close to our proposed detector but has worse performance for the same number of iterations. The reason behind this is that the full-rank MSER converges slower than JP-MSER as the number of relays increases.

Fig. 3.5 plots the BER of the two-way cooperative communication system when communicating over Rayleigh fading channel. The detector is able to keep up with the Ml detector for any number of relays , i.e., it is able to achieve higher orders of

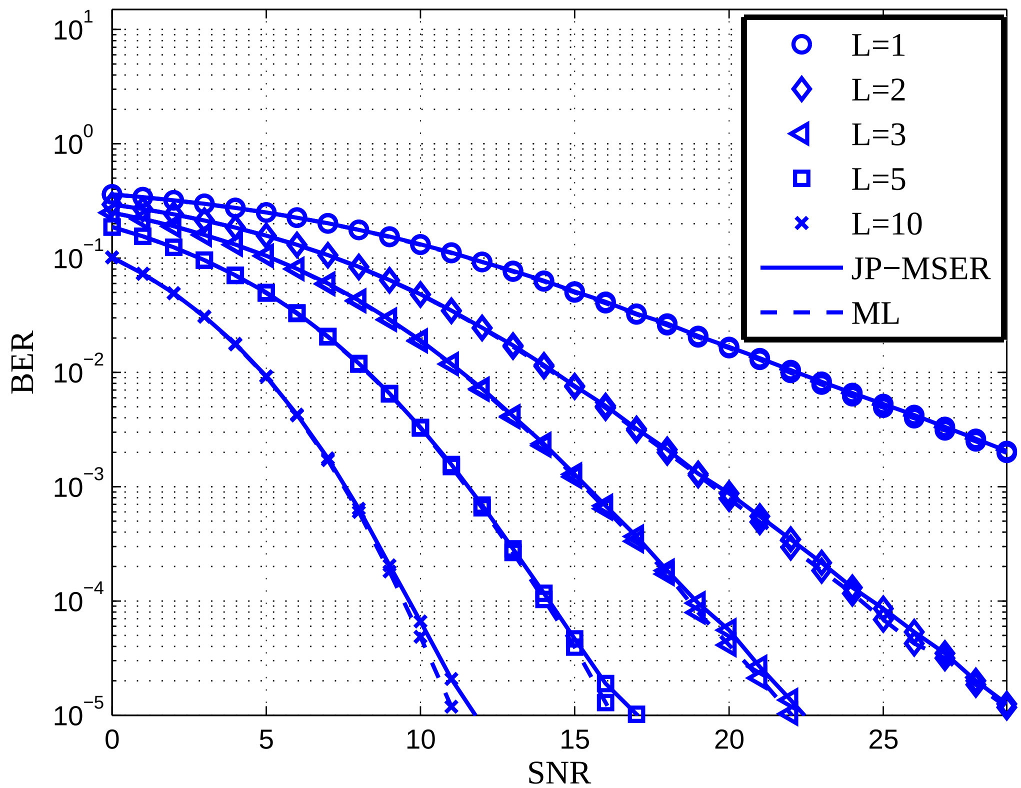


Figure 3.5: BER vs. SNR performance for the proposed detector with two-way relaying across different values of $L$.

diversity. In the detection phase, the step-sizes are calculated as $\mu = 0.2$ and $\eta = 3$ using appropriate convergence curves. The figure shows the benefits of using this detector as it hits the ML detector and also has lower complexity than other sub-optimal detectors as shown in Table 3.1. In Fig. 3.6, we show the effect of changing the doppler frequency on our detector. The detector hits ML for a normalized doppler of 0.0001 but lags behind ML for higher values while still performing adequately.

Finally, the complexity of our proposed algorithm is compared to the other detectors in Fig. 3.7. The complexity computations are shown in Table 3.1. These computations assume QPSK modulation and this is why the ML detector has lower complexity than CS. It can be seen that for large $L$, CS has the highest complexity across all other detectors. Our proposed BER detector has a low complexity that is

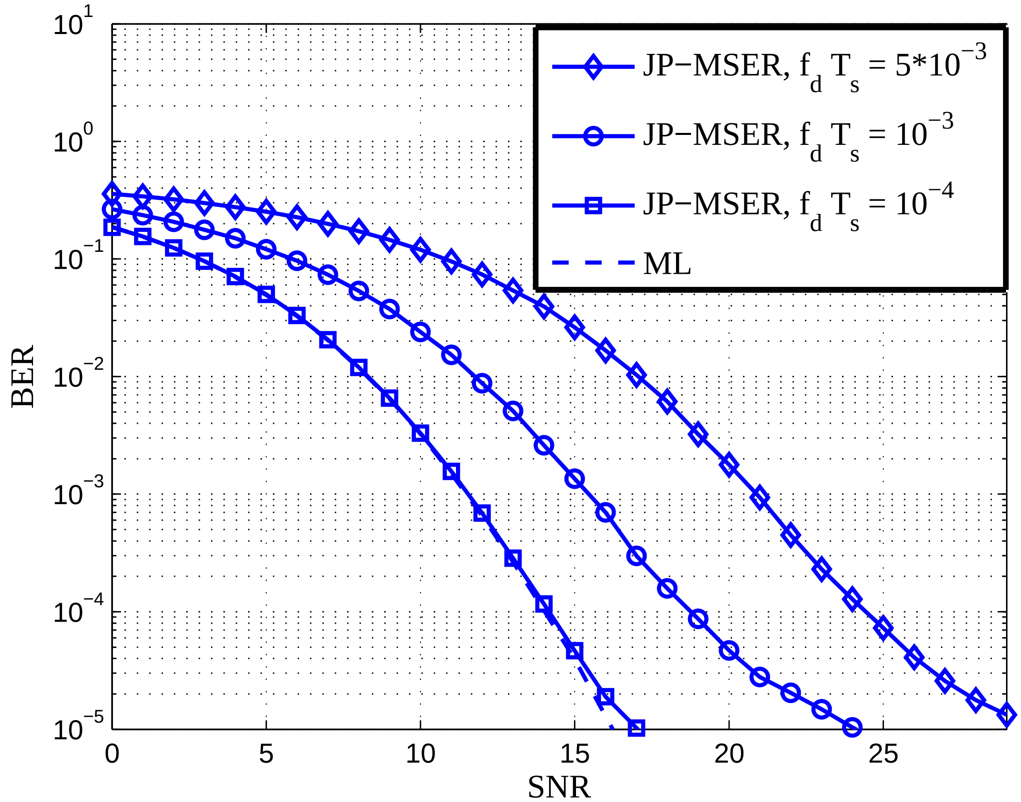


Figure 3.6: BER vs. SNR performance for the proposed detector with two-way relaying with different doppler frequencies.

also comparable to the TPA complexity, but BER increases linearly in $U$ while TPA increases quadratically in $U$, allowing a larger $U$ for our detector without adding much complexity.

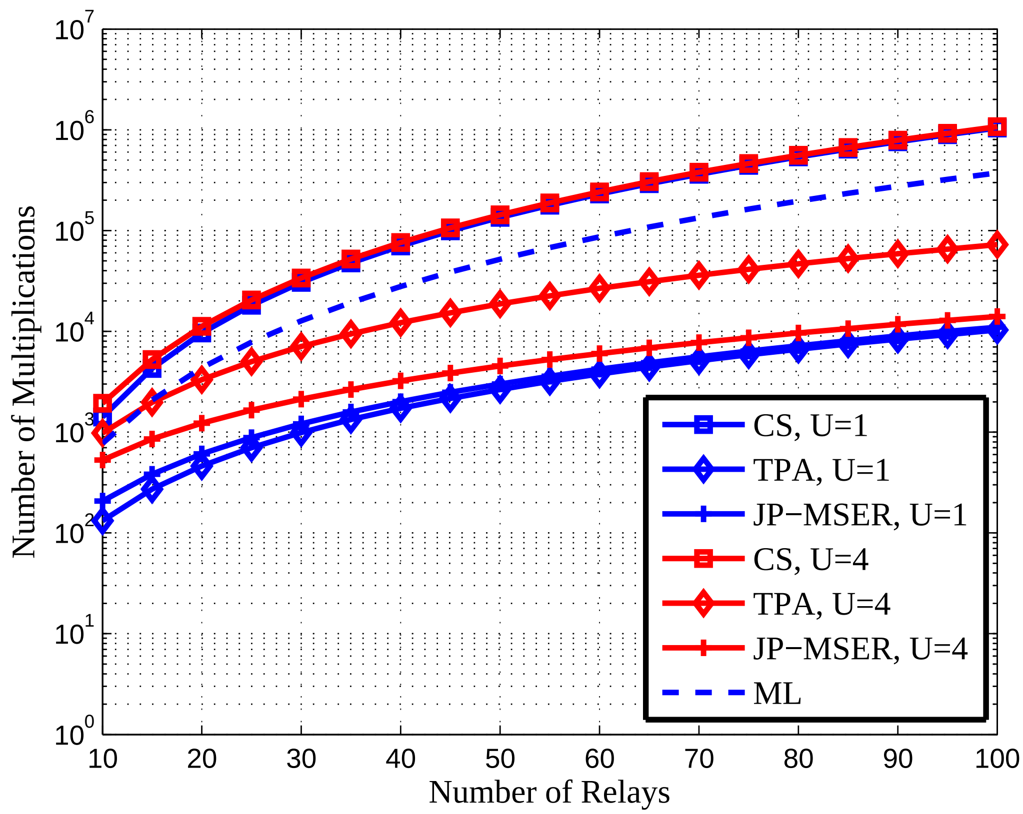


Figure 3.7: Number of multiplications versus the size of the system $L$ for different detectors and $U$'s.

# Chapter 4

# Concluding Remarks

## 4.1 Summary

In Chapter 2 of this thesis, an efficient MSE-based detector for cooperative communication systems with one-way relaying is proposed. This threshold based adaptive detector only requires the knowledge of training symbols to determine the optimal MSE. The proposed algorithm achieves a similar MSE performance as that of the JIO but with a lower $U$. Furthermore, by introducing a tolerable difference in MSE, the constraint on $U$ is relaxed, which enhances complexity savings at the expense of MSE performance. The proposed algorithm exhibits the classic convergence properties with respect to step-size. Lastly in the first part, the thesis showed that the algorithm works when there is a channel estimation error.

In Chapter 3 of the thesis, a novel JP-MSER detector is proposed for one-way and two-way cooperative communication systems that are limited in training. The detector hits the ML detector performance for lower values of $U$ as compared to the TPA-based MMSE detector. The detector has lower complexity as compared to SC-, CS-, and TPA-based MMSE detectors, and is superior to all of them. We designed a novel preprocessing matrix that allowed our detector to converge faster than the full-rank MSER detector when the system size $L$ is large. Finally, we dropped the

CSI requirement and estimated the channel using training symbols.

## 4.2 Future Research Work

The work presented in the second part dealt with small constellations such as binary phase shift keying (BPSK) and QPSK. The challenging task ahead is to extend the work to higher modulation schemes such as Quadrature Amplitude Modulation (QAM). Later we plan to tackle the case of multi-input multi-output (MIMO) systems and check how our algorithms work under such conditions.

# REFERENCES


[1] A. Sendonaris, E. Erkip, and B. Aazhang, "User cooperation diversity. part i. system description," *IEEE Transactions on Communications*, vol. 51, no. 11, pp. 1927–1938, Nov. 2003.

[2] R. U. Nabar, H. Bolcskei, and F. W. Kneubuhler, "Fading relay channels: Performance limits and space-time signal design," *IEEE Journal on Selected Areas in Communications*, vol. 22, no. 6, pp. 1099–1109, Jun. 2004.

[3] P. Larsson, N. Johansson, and K.-E. Sunell, "Coded bi-directional relaying," *VTC 2006-Spring. IEEE 63rd Vehicular Technology Conference, 2006.*, vol. 2, pp. 851–855, May 2006.

[4] A. Sendonaris, E. Erkip, and B. Aazhang, "User cooperation diversity. part ii. implementation aspects and performance analysis," *IEEE Transactions on Communications*, vol. 51, no. 11, pp. 1939–1948, Nov. 2003.

[5] R. Krishna, Z. Xiong, and S. Lambotharan, "A cooperative MMSE relay strategy for wireless sensor networks," *IEEE Signal Processing Letters*, vol. 15, pp. 549–552, Jul. 2008.

[6] N. Khajehnouri and A. Sayed, "Distributed MMSE relay strategies for wireless sensor networks," *IEEE Transactions on Signal Processing*, vol. 55, no. 7, pp. 3336–3348, Jul. 2007.

[7] Y. Chen and Q. Zhao, "On the lifetime of wireless sensor networks," *IEEE Communications Letters*, vol. 9, no. 11, pp. 976–978, Nov. 2005.

[8] Y. Hou, Y. Shi, H. Sherali, and S. Midkiff, "On energy provisioning and relay node placement for wireless sensor networks," *IEEE Transactions on Wireless Communications*, vol. 4, no. 5, pp. 2579–2590, Sep. 2005.

[9] J. Laneman, D. Tse, and G. W. Wornell, "Cooperative diversity in wireless networks: Efficient protocols and outage behavior," *IEEE Transactions on Information Theory*, vol. 50, no. 12, pp. 3062–3080, Dec. 2004.

[10] A. Bletsas, A. Khisti, D. Reed, and A. Lippman, "A simple cooperative diversity method based on network path selection," *IEEE Journal on Selected Areas in Communications*, vol. 24, no. 3, pp. 659–672, Mar. 2006.

[11] S. Hussain, M.-S. Alouini, and M. Hasna, "A diversity compression and combining technique based on channel shortening for cooperative networks," *IEEE Transactions on Wireless Communications*, vol. 11, no. 2, pp. 659–667, Feb. 2012.

[12] Q. Z. Ahmed, K. Park, M. Alouini, and S. Aissa, "Compression and combining based on channel shortening and rank reduction technique for cooperative wireless sensor networks," *IEEE Transactions on Vehicular Technology*, vol. 63, no. 1, pp. 72–81, Jan. 2014.

[13] B. Gedik and M. Uysal, "Impact of imperfect channel estimation on the performance of amplify-and-forward relaying," *IEEE Transactions on Wireless Communications*, vol. 8, no. 3, pp. 1468–1479, Mar. 2009.

[14] S. S. Ikki, "Performance analysis of cooperative diversity networks with imperfect channel estimation over rician fading channels," *IET Signal Processing*, vol. 6, no. 6, pp. 577–583, Aug. 2012.

[15] O. Amin, S. S. Ikki, and M. Uysal, "On the performance analysis of multirelay cooperative diversity systems with channel estimation errors," *IEEE Transactions on Vehicular Technology*, vol. 60, no. 5, pp. 2050–2059, June 2011.

[16] Y. Zhang, H. Zhao, and C. Pan, "Optimization of an amplify-and-forward relay network considering time delay and estimation error in channel state information," *to appear in IEEE Transactions on Vehicular Technology*, pp. 1–6, Nov. 2013.

[17] R. De Lamare and R. Sampaio-Neto, "Adaptive reduced-rank equalization algorithms based on alternating optimization design techniques for mimo systems,"

*IEEE Transactions on Vehicular Technology*, vol. 60, no. 6, pp. 2482–2494, Jun. 2011.

[18] R. D. Lamare and R. Sampaio-Neto, "Reduced-rank adaptive filtering based on joint iterative optimization of adaptive filters," *IEEE Signal Processing Letters*, vol. 14, no. 12, pp. 980–983, Dec. 2007.

[19] M.-S. Alouini, A. Scaglione, and G. Giannakis, "Pcc: principal components combining for dense correlated multipath fading environments," *IEEE-VTS Fall VTC 2000. 52nd Vehicular Technology Conference.*, vol. 5, pp. 2510–2517 vol.5, 2000.

[20] J. S. Goldstein and I. S. Reed, "Reduced-rank adaptive filtering," *IEEE Transactions on Signal Processing*, vol. 45, no. 2, pp. 492–496, Feb. 1997.

[21] B. Rankov and A. Wittneben, "Spectral efficient protocols for half-duplex fading relay channels," *IEEE Journal on Selected Areas in Communications*, vol. 25, no. 2, pp. 379–389, Feb. 2007.

[22] Y. Han, S. H. Ting, C. K. Ho, and W. H. Chin, "Performance bounds for two-way amplify-and-forward relaying," *IEEE Transactions on Wireless Communications*, vol. 8, no. 1, pp. 432–439, Jan. 2009.

[23] K.-S. Hwang, Y.-C. Ko, and M.-S. Alouini, "Performance analysis of two-way amplify and forward relaying with adaptive modulation over multiple relay network," *IEEE Transactions on Communications*, vol. 59, no. 2, pp. 402–406, Feb. 2011.

[24] H. Guo, J. Ge, and H. Ding, "Symbol error probability of two-way amplify-and-forward relaying," *IEEE Communications Letters*, vol. 15, no. 1, pp. 22–24, Jan. 2011.

[25] C. Sun and C. Yang, "Is two-way relay more energy efficient?" *2011 IEEE Global Telecommunications Conference (GLOBECOM 2011)*, pp. 1–6, Dec. 2011.

[26] S. Chen, S. Tan, L. Xu, and L. Hanzo, "Adaptive minimum error-rate filtering design: A review," *Elsevier Signal Processing*, vol. 88, no. 7, pp. 1671 – 1697,

July 2008. [Online]. Available: http://www.sciencedirect.com/science/article/pii/S0165168408000091

[27] Q. Ahmed, M.-S. Alouini, and S. Aissa, "Bit error-rate minimizing detector for amplify-and-forward relaying systems using generalized gaussian kernel," *IEEE Signal Processing Letters*, vol. 20, no. 1, pp. 55–58, Jan. 2013.

[28] Q. Ahmed, K.-H. Park, M.-S. Alouini, and S. Aissa, "Optimal linear detectors for nonorthogonal amplify-and-forward protocol," *2013 IEEE International Conference on Communications (ICC)*, pp. 4829–4833, June 2013.

[29] A. Chowdhery and R. Mallik, "Linear detection for the nonorthogonal amplify and forward protocol," *IEEE Transactions on Wireless Communications*, vol. 8, no. 2, pp. 826–835, Feb. 2009.

[30] M. Gong, F. Chen, H. Yu, Z. Lu, and L. Hu, "Normalized adaptive channel equalizer based on minimal symbol-error-rate," *IEEE Transactions on Communications*, vol. 61, no. 4, pp. 1374–1383, Apr. 2013.

[31] S.-H. Choi, J.-S. Baek, J.-S. Han, and J.-S. Seo, "Channel estimations using extended orthogonal codes for AF multiple-relay networks over frequency-selective fading channels," *IEEE Transactions on Vehicular Technology*, vol. 63, no. 1, pp. 417–423, Jan. 2014.

[32] F. Gao, T. Cui, and A. Nallanathan, "On channel estimation and optimal training design for amplify and forward relay networks," *IEEE Transactions on Wireless Communications*, vol. 7, no. 5, pp. 1907–1916, May 2008.

[33] C. Patel and G. Stuber, "Channel estimation for amplify and forward relay based cooperation diversity systems," *IEEE Transactions on Wireless Communications*, vol. 6, no. 6, pp. 2348–2356, Jun. 2007.

[34] C.-L. Wang, J.-Y. Chen, and H.-C. Wang, "Capacity analysis and power allocation under imperfect channel estimation for af-based cooperative relay systems," *2012 IEEE Global Communications Conference (GLOBECOM)*, pp. 4677–4682, Dec. 2012.

[35] Y. Zhao, R. Adve, and T. J. Lim, "Improving amplify-and-forward relay networks: optimal power allocation versus selection," *IEEE Transactions on Wireless Communications*, vol. 6, no. 8, pp. 3114–3123, Aug. 2007.

[36] D. Chen and J. Laneman, "Cooperative diversity for wireless fading channels without channel state information," *Conference Record of the Thirty-Eighth Asilomar Conference on Signals, Systems and Computers, 2004.*, vol. 2, pp. 1307–1312 Vol.2, Nov. 2004.

[37] S. Verdu, *Multiuser Detection*, ser. Cambridge U.K. Cambridge University Press, 1998.

[38] S. Haykin, *Adaptive Filter Theory*, ser. Prentice-Hall Information and System Sciences Series. Prentice Hall, 2002. [Online]. Available: http://books.google.ie/books?id=eMcZAQAAIAAJ

[39] Q. Ahmed, M.-S. Alouini, and S. Aissa, "A minimum bit error-rate detector for amplify and forward relaying systems," *2012 IEEE 75th Vehicular Technology Conference (VTC Spring)*, pp. 1–5, May 2012.

[40] C.-L. Wang, T.-N. Cho, and K.-J. Yang, "On power allocation and relay selection for a two-way amplify-and-forward relaying system," *IEEE Transactions on Communications*, vol. 61, no. 8, pp. 3146–3155, Aug. 2013.

[41] M. K. Simon and M.-S. Alouini, *Digital Communication over Fading Channels*, ser. Wiley Series in Telecommunications and Signal Processing. Wiley Series, 2005.

# APPENDIX

# A Papers Accepted and Under Review

• A. Abuzaid, Q. Z. Ahmed, M.-S. Alouini, "Threshold-based Detection for Amplify-and-Forward Cooperative Communication Systems with Channel Estimation Error", in Proceedings of IEEE 80th Vehicular Technology Conference (VTC Fall 2014), Vancouver, Canada, Sep. 2014.

• A. Abuzaid, Q. Z. Ahmed, M.-S. Alouini, "Joint Preprocesser-Based Detector for Cooperative Networks with Hardware Constraint", Under review in IEEE Signal Processing Letters, Apr. 2014.